WL-TR-95-2141

ELECTROCHEMICAL PROPERTIES OF PEO:$LiBF_4$-Li_3N COMPOSITE ELECTROLYTES

B. Kumar and J. Schaffer

University of Dayton
Research Institute
300 College Park
Dayton OH 45469-0170

December 1995

Interim Report for period June 1, 1993-May 31, 1995

AERO PROPULSION & POWER DIRECTORATE
WRIGHT LABORATORY
AIR FORCE MATERIAL COMMAND
WRIGHT-PATTERSON AIR FORCE BASE, OHIO 45433-7251

NOTICE

When Government drawings, specifications, or other data are used for any purpose other than in connection with a definitely Government-related procurement, the United States Government incurs no responsibility or any obligation whatsoever. The fact that the Government may have formulated or in any way supplied the said drawings, specifications, or other data, is not to be regarded by implication, or otherwise in any manner construed, as licensing the holder, or any other person or corporation; or as conveying any rights or permission to manufacturer, use, or sell any patented invention.

This report is releasable to the National Technical Information Service (NTIS). At NTIS, it will be available to the general public, including foreign nationals.

This technical report has been reviewed and is approved for publication.

LAWRENCE G. SCANLON
Project Engineer

RICHARD A. MARSH
Technical Area Manager
Battery Electrochemistry Laboratory
Power Technology Branch

MICHAEL D. BRAYDICH, Lt.Col., USAF
Deputy Director
Aerospace Power Division
Aero Propulsion & Power Directorate

If your address has changed, if you wish to be removed from our mailing list, or if the addressee is no longer employed by your organization, please notify WL/POOC, WPAFB, OH 45433-7251 to help us maintain a current mailing list.

Copies of this report should not be returned unless return is required by security considerations, contractual obligations, or notice on a specific document.

REPORT DOCUMENTATION PAGE

Form Approved
OMB No. 0704-0188

1. AGENCY USE ONLY *(Leave blank)*	2. REPORT DATE	3. REPORT TYPE AND DATES COVERED
	December 1995	FINAL June 1, 1993-May 31, 1995

4. TITLE AND SUBTITLE

Electrochemical Properties of PEO:$LiBF_4$-Li_3N Composite Electrolytes

5. FUNDING NUMBERS

F33615-93-C-2350
PE 61102F
PR 2303
TA P4
WU 00

6. AUTHOR(S)

B. Kumar and J. Schaffer

7. PERFORMING ORGANIZATION NAME(S) AND ADDRESS(ES)

University of Dayton Research Institute
300 College Park
Dayton, OH 45469-0170

8. PERFORMING ORGANIZATION REPORT NUMBER

UDR-TR-95-121

9. SPONSORING/MONITORING AGENCY NAME(S) AND ADDRESS(ES)

AERO PROPULSION & POWER DIRECTORATE
WRIGHT LABORATORY
AIR FORCE MATERIAL COMMAND
WRIGHT-PATTERSON AIR FORCE BASE, OHIO 45433-7251

10. SPONSORING/MONITORING AGENCY REPORT NUMBER

WL-TR-95-2141

11. SUPPLEMENTARY NOTES

N/A

12a. DISTRIBUTION/AVAILABILITY STATEMENT

Approved for public release; distribution is unlimited

12b. DISTRIBUTION CODE

13. ABSTRACT *(Maximum 200 words)*

A processing technique to produce ≅100 μm thick films of PEO:$LiBF_4$-Li_3N composite electrolyte was developed. The electrochemical properties of the film were found to be sensitive to annealing temperature and time.

The ac impedance technique was used to characterize the composite films. At low concentrations of Li_3N, the electrolytes exhibited interpretable ac impedance spectra; however, at higher Li_3N concentrations the spectra were complex. Nonetheless, the general observation was that the increasing concentration of Li_3N increased the conductivity of the composite electrolyte.

Annealing the specimens in 125-140°C temperature range yields high conductivity material. The reproductability of the specimen preparation and conductivity data is excellent.

Characterization of the specimen using DSC, TGA x-ray diffraction, and infrared spectroscopy reveal that a high temperature (125-145°C) annealing leads to formation of a new phase which is believed to be the high conductivity phase.

Cyclic voltammograms obtained from the composite electrolyte material reveal that these materials are stable when in contact with lithium. A symmetric Li/composite electrolyte/Li cell was cycled successfully for 150 cycles with a current density of 100μA cm^{-2}

~~14. SUBJECT TERMS~~

Polymer Electrolyte Composite Electrolyte

15. NUMBER OF PAGES

48

16. PRICE CODE

17. SECURITY CLASSIFICATION OF REPORT	18. SECURITY CLASSIFICATION OF THIS PAGE	19. SECURITY CLASSIFICATION OF ABSTRACT	20. LIMITATION OF ABSTRACT
Unclassified	Unclassified	Unclassified	UL

TABLE OF CONTENTS

Section		Page
1	INTRODUCTION	1
2	EXPERIMENTAL	3
	2.1 Preparation of Composite Films	3
	2.2 Conductivity Measurement by an AC Technique	3
3	RESULTS AND DISCUSSION	4
	3.1 Electrochemical Properties of Composite Electrolytes	4
	3.2 Effect of Annealing	16
	3.3 Thermogravimetric Analysis (TGA)	26
	3.4 Differential Scanning Calorimetry (DSC)	26
	3.5 X-ray Diffraction	31
	3.6 Infrared Spectroscopy	31
	3.7 Effect of Li_3N Particle Size	37
	3.8 Effect of Li_3N on Conductivity of the Composite Electrolyte	37
	3.9 Theoretical Basis for Conductivity Enhancement in Li_3N-PEO:$LiBF_4$ Composites	40
	3.10 Conductivity of Over-Annealed Specimens	43
4	SUMMARY AND CONCLUSIONS	47
5	REFERENCES	48

LIST OF ILLUSTRATIONS

Figure		Page
1	Log σ vs 1/T for PEO:$LiBF_4$ - 5 wt% Li_3N Composite Electrolyte.	6
2	Cyclic Voltammogram of PEO:$LiBF_4$-5 wt% Li_3N specimen at 60°C with a Scan Rate of 5 mVS^{-1} (electrode area = 0.65 cm^2).	7
3	Cyclic Voltammogram of PEO:$LiBF_4$-5 wt% Li_3N specimen at 60°C with a Scan Rate of 10 mVS^{-1} (electrode area = 0.65 cm^2).	8
4	AC Impedance of a PEO:$LiBF_4$-25% Li_3N Material at 90°C.	10
5	Temperature Dependence of Conductivity of PEO:$LiBF_4$-25% Li_3N Solid Electrolyte Material.	11
6	Log σ vs 1/T for PEO:$LiBF_4$-40% Li_3N Annealed at 125°C Overnight.	12
7	Log σ vs 1/T of PEO:$LiBF_4$-40% Li_3N electrolyte. The batch materials were pulverized before making the film. The film was annealed at 125°C.	13
8	Cyclic Voltammogram of PEO:$LiBF_4$-40% Li_3N Material at 30.2°C and a Scan Rate of 1 mVS^{-1}.	14
9	Cyclic Voltammogram of PEO:$LiBF_4$-40% Li_3N Material at 30.2°C and a Scan Rate of 2 mVS^{-1}.	15
10	Log σ vs 1/T for PEO:$LiBF_4$-50% Li_3N Material Annealed at 100°C for 48 hours.	17
11	Log σ vs 1/T for PEO:$LiBF_4$-Li_3N Composite Electrolyte Annealed at 125°C.	18
12	AC Impedance Spectrum of PEO:$LiBF_4$-60 wt% Li_3N Composite Electrolyte at 15°C.	19
13	Cyclic Voltammogram of the Li/Composite/Li Cell (Li_3N=60%) at 25°C and Sweep Rate of 2 mVS^{-1}.	20
14	Conductivity of PEO:$LiBF_4$-60% Li_3N Material Annealed at 90°C and 125°C.	23
15	Conductivity Data of PEO:$LiBF_4$-60% Li_3N Material Annealed at 125°C and Then Additionally Annealed at 125°C and 135°C.	24
16	Conductivity Data of PEO:$LiBF_4$-60% Li_3N Material Annealed at 24 hrs and 72 hrs, respectively	25
17	TGA Curve of As-Prepared PEO:$LiBF_4$-60 wt% Li_3N Specimen (a).	27
18	TGA Curve of PEO:$LiBF_4$-Li_3N Specimen (b) - Annealed at 90°C.	28
19	TGA Curve of PEO:$LiBF_4$-Li_3N Specimen (c)- Annealed at 145°C.	29

LIST OF ILLUSTRATIONS (Concluded)

Figure		Page
20	DSC Curve of PEO:$LiBF_4$-60 wt% Li_3N Specimen (a) - As Prepared.	30
21	DSC Curve of PEO:$LiBF_4$-60 wt% Li_3N Specimen (b) - Annealed at 90°C for 24 hrs..	32
22	DSC Curve of PEO:$LiBF_4$-60 wt% Li_3N Specimen (c) - Annealed at 145°C for 24 hrs.	33
23	X-ray Diffraction Patterns of (a) PEO:$LiBF_4$-60 wt% Li_3N as-prepared, (b) PEO:$LiBF_4$-60 wt% Li_3N - annealed at 90°C for 24 hrs, and (c) PEO:$LiBF_4$-60 wt% Li_3N - annealed at 145°C for 24 hrs.	34
24	Effect of Particle Size on Conductivity in PEO:$LiBF_4$-40 wt% Li_3N Material.	38
25	Effect of Li_3N Particle Size on Conductivity in PEO:$LiBF_4$-60 wt% Li_3N Material.	39
26	Log σ vs 1/% Plots of PEO:$LiBF_4$, and 5, 25, and 40 wt% Li_3N Materials.	42
29	Conductivity of Li_3N-PEO:$LiBF_4$ Composite Electrolyte vs Volume Fraction of Li_3N.	45

LIST OF TABLES

Table		Page
1	Conductivity (σ) of Annealed and Unannealed PEO:$LiBF_4$ - 5 wt% Li_3N Composite Electrolytes	5
2	Temperature Dependence of Conductivity (σ) of PEO:$LiBF_4$- 25 wt% Li_3N Composite Electrolytes Annealed at Various Temperatures and Times	21
3	d-spacings of PEO-60 wt% Li_3N Composite Specimens	35
4	IR Absorption Bands in Li_3N, $LiBF_4$, PEO, PEO:$LiBF_4$, and 60% Li_3N Material Heat Treated at 145°C	36
5	Composition and Properties of PEO:$LiBF_4$/Li_3N Composite Electrolytes	41
6	Conductivity and Diffusion Coefficients of Li_3N, PEO:$LiBF_4$, and Composite Electrolytes	44

1. INTRODUCTION

Solid polymer electrolytes have attracted a great deal of interest in the last decade. The major driving force for this interest is a technological application - rechargeable and long life-cycle power sources. The research efforts of the last decade have contributed significantly toward the definition of issues and the state-of-understanding of solid polymer electrolytes. Issues such as ambient temperature conductivity, cationic transport number, electrode-electrolyte interfacial reactions, and lithium recyclability remain matters of significant concern. Thus, it is not surprising that most of the recent research reports address these issues.

In the last 4 years, two approaches to enhance the room temperature conductivity of polymer composite electrolytes have been reported. The first approach makes use of a highly conductive liquid phase in a polymer matrix,[1] frequently referred to as gel electrolytes. Due to the presence of a liquid phase, these electrolytes exhibit room temperature conductivity in the 10^{-2}-10^{-3} S cm^{-1} range. The basis of the second approach is the incorporation of solid inorganic additives or fillers in the conducting polymers.[2,3,4] Conductivity enhancement occurs at low temperatures; however, the conductivity of this type of solid electrolyte material is not as high as those made by the first approach. Basically, both approaches produce composite electrolyte materials, the difference being the fact that the gel type electrolyte consists of a solid polymer and a highly conductive liquid phase whereas in the second type of electrolyte, both the polymer and inorganic additive are solids.

Capuano, et al.[3] reported that the incorporation of γ-Al_2O_3 and $LiAlO_2$ in the PEO polymer increases room temperature conductivity by an order of magnitude. Similar observations were reported when zeolite was introduced in the PEO:$LiBF_4$ complex.[5] There was no increase in room temperature conductivity when a lithium borosulfate glass was incorporated in a PEO:$LiBF_4$ complex; however, the charge transfer resistance decreased by a factor of three due to a small addition of the glass.[6]

The ionic conductivity of single crystal Li_3N has been reported to be of the order of 10^{-3} S cm^{-1} around ambient temperature.[7] Due to the brittleness of the material, its application in thin film forms in electrochemical devices is not viable. An exploratory attempt to evaluate the properties of Li_3N polymer composites has been reported by Skaarup, et al.[8] These authors stated that at small volume percentages (5-10%) of polymer, the room temperature conductivity of composite electrolytes is about a factor of 1,000 larger than that of the pure polymer, and the activation energy for conduction is approximately equal to the activation energy for lithium ion conduction in Li_3N. However, these authors conducted experimental studies on rather thick films, 0.5-0.6 mm. Yang, et al.[9] reported that the decomposition voltage of Li_3N exceeds 5 V

due to a kinetic barrier in the formation of elementary nitrogen from two N^{3+} ions in the Li_3N lattice. In addition, the free energy of formation of Li_3N is -30.81 Kcal mol^{-1} and is reported to be thermodynamically stable when in contact with lithium.[7] These desirable electrochemical attributes of Li_3N motivated the present work on composite electrolytes. The polymer component of the composite has the potential to facilitate the fabrication of thin films while the Li_3N phase will provide the needed electrochemical performance. This investigation particularly focuses on the conductivity issue and reports the attributes of PEO:$LiBF_4$-Li_3N composite electrolytes.

2. EXPERIMENTAL

2.1 Preparation of Composite Films

The composite films were made using reagent grade poly(ethylene) oxide (PEO), lithium tetrafluoroborate ($LiBF_4$), and lithium nitride (Li_3N). Li_3N with a particle size of 250 μm was obtained from Johnson Matthey. This Li_3N was further ground to 25-100 μm size range for use in the formulation of composite electrolytes. The PEO:$LiBF_4$ proportion was used such that the oxygen to lithium ratio was maintained at 8:1. Initially, these components were mixed and ground in a mortar and pestle. The PEO was introduced in small portions in order to prevent the massive aggregation of the batch materials during the grinding operation. The percentage of lithium nitride varied from 0 to 60% by wt. A portion of the ground mixture was placed in a die between two teflon films. The ground mixture was compacted in a Carver Press at temperatures ranging from 80 to 125°C for about 10 minutes. The pressure was also varied from 1,000 - 20,000 psig. The compacting parameters, i.e., temperature, pressure, and time depended upon the composition of the composite electrolyte. Generally, the compacting temperature, pressure, and time, were raised as the concentration of Li_3N increased. After compacting the mixture, the die was removed from the press and allowed to cool for about 20 min. The compacted composite disc was then removed, further thinned on a hot plate between two sheets of teflon, and flattened with a roller. The electrolyte film thus prepared varied in thickness from 0.07-0.15 mm.

2.2 Conductivity Measurement by AC Technique

Symmetric cells with blocking (SS/CE/SS*) and nonblocking (Li/CE/Li) configurations were constructed. These cells were contained in an air-tight glass vessel with electrical connections. The composite electrolyte film contained in the cell was annealed between 60-145°C in a helium atmosphere. After annealing the film, electrochemical measurements were conducted in the temperature range of 0-100°C using EG&G Electrochemical System (Model 273A) interfaced with an IBM-compatible computer.

---

* SS = stainless steel
CE = composite electrolyte

3. RESULTS AND DISCUSSION

The electrochemical data obtained from various specimens are compiled and presented for various amounts of Li_3N in the composite electrolyte. Initially, these materials will be examined separately, then a collective analysis on the effect of Li_3N on the properties of composite electrolytes will be presented.

3.1 Electrochemical Properties of Composite Electrolytes

1. PEO:$LiBF_4$ - 5% Li_3N Material

The ac impedance data were collected from the as-prepared films which exhibit low conductivity and is similar to data obtained from the PEO:$LiBF_4$ (0:Li=8) material. After annealing the film at 60°C overnight, its conductivity increased by over an order of magnitude. Table 1 presents the conductivity data at various temperatures for unannealed and annealed specimens. Although the conductivity of the annealed specimens at 30°C appears to be slightly higher than that of the PEO:$LiBF_4$ materials, the effect of the 5% Li_3N does not appear to be pronounced and significant. The temperature dependence of the conductivity of the material is shown in Figure 1. The conductivity shows Arrhenius type behavior with an activation energy of 27.61 kcal $mole^{-1}$. The activation energy is typical of the PEO:$LiBF_4$ type of materials, and, thus, it may be inferred that the addition of 5% Li_3N has done little to change the basic mechanism of the conduction process.

The cyclic voltammograms obtained from Li/composite/Li cells at the scan rates of 5 and 10 mV S^{-1} are shown in Figures 2 and 3, respectively. These voltammograms reveal the deposition and stripping characteristics of lithium on a lithium working electrode. The counter and reference electrodes were the same. Figure 2 shows a symmetric anodic and cathodic peak with current densities of about 1 mA cm^{-2}. The voltammogram suggests identical deposition and stripping characteristics similar to those of lithium on a lithium electrode. After the scan rate was increased to 10 mV S^{-1}, anodic and cathodic peaks exhibited dissimilar characteristics, implying passivation of the lithium electrode. Both voltammograms indicated that the electrolyte material is stable in a voltage window of approximately ±2 V.

2. PEO:$LiBF_4$ - 25% Li_3N Material

The concentration of Li_3N was increased to 25 wt% while employing the same processing technique similar to the 5% Li_3N material.

TABLE 1

Conductivity (σ) of Annealed and Unannealed

PEO:$LiBF_4$ - 5% Li_3N Composite Electrolyte

Temperature (°C)	Unannealed	Annealed
0	5.23×10^{-11} S cm^{-1}	3.26×10^{-9} S cm^{-1}
15	2.03×10^{-9} S cm^{-1}	3.73×10^{-8} S cm^{-1}
30	3.54×10^{-8} S cm^{-1}	2.74×10^{-7} S cm^{-1}
45	---	3.43×10^{-6} S cm^{-1}
60	---	3.44×10^{-5} S cm^{-1}

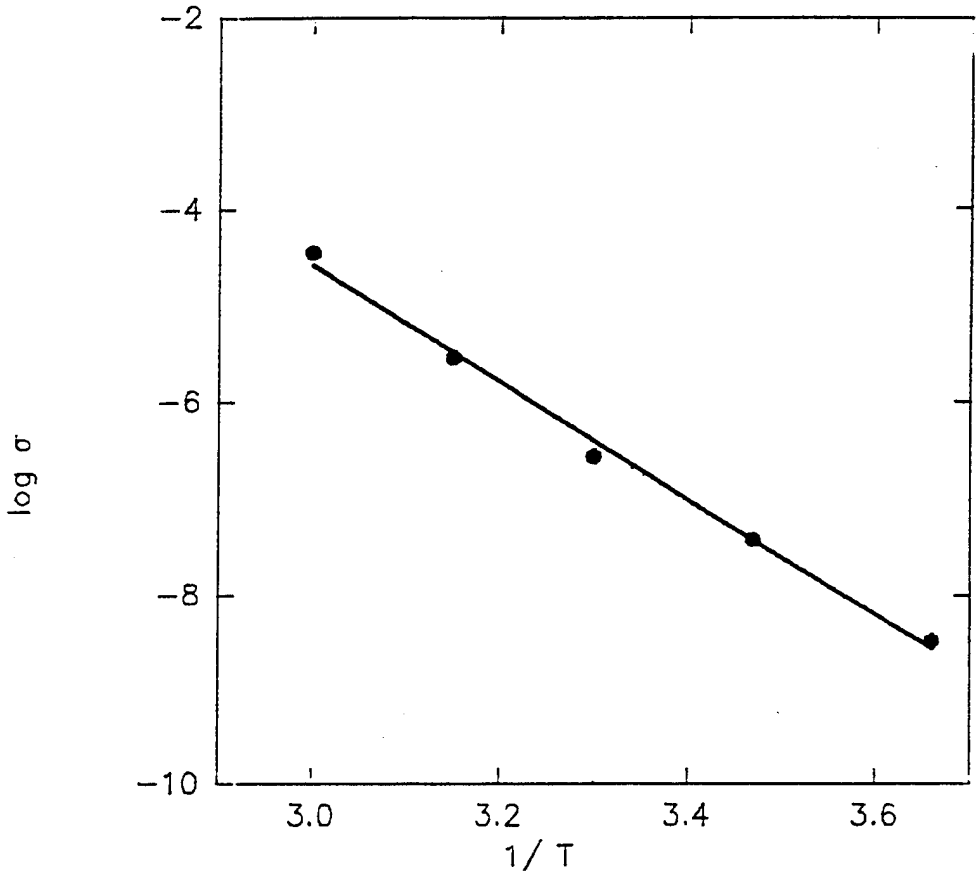

Figure 1. Logσ vs 1/T for PEO:$LiBF_4$ - 5 wt% Li_3N Composite Electrolyte.

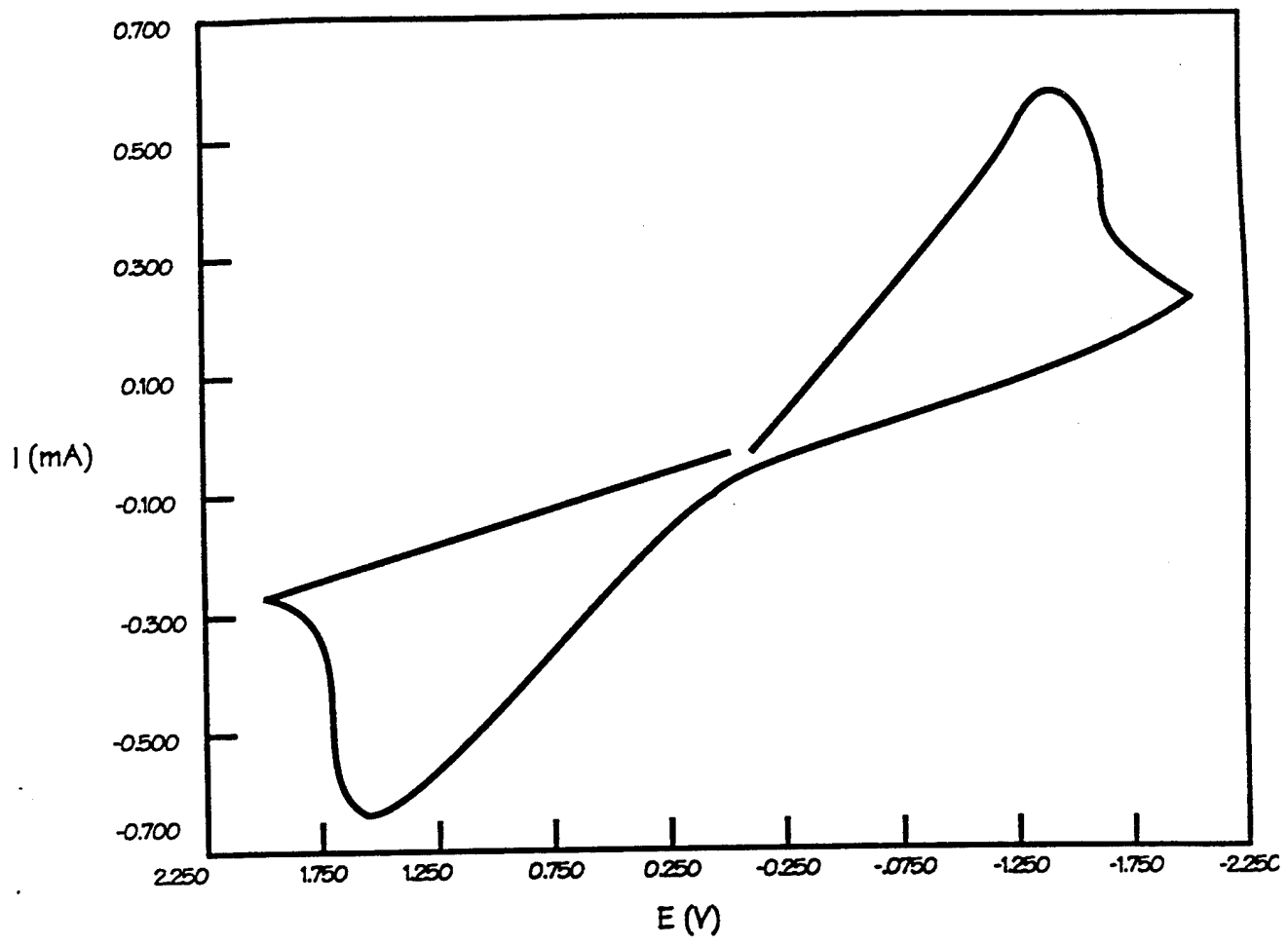

Figure 2. Cyclic Voltammogram of PEO:$LiBF_4$-5 wt% Li_3N specimen at 60°C with a Scan Rate of 5 mVS^{-1} (electrode area=0.65 cm^2).

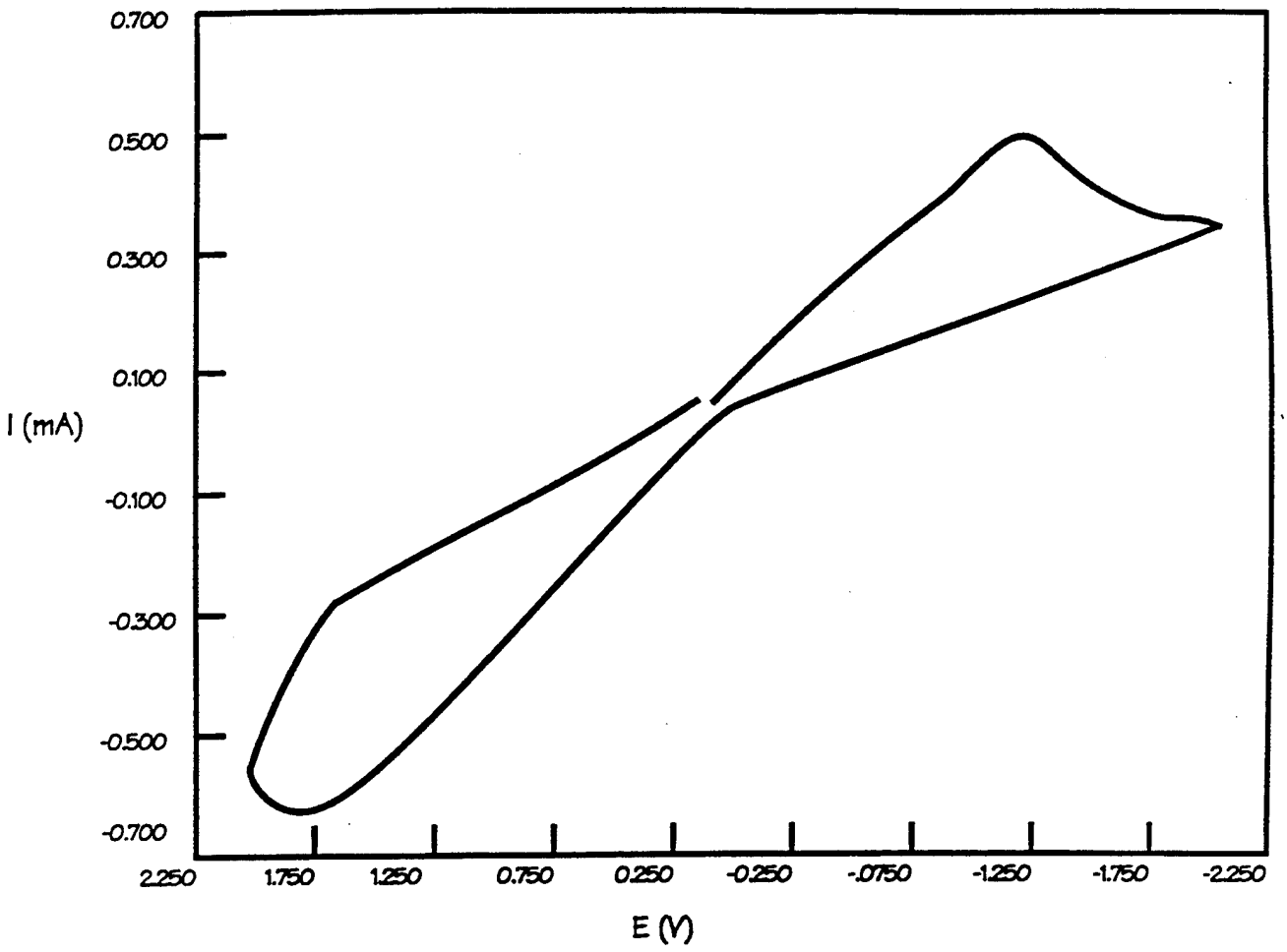

Figure 3. Cyclic Voltammogram of PEO:$LiBF_4$-5 wt% Li_3N specimen at 60°C with a Scan Rate of 10 mVS^{-1}(electrode area=0.65 cm^2).

One of the central features of this material was its nonsemicircular complex impedance plane diagram typical to that shown in Figure 4. The linear segment, toward the high frequency side, intersects the z' axis at some nonzero value. This value was used as the resistance of the electrolyte from which conductivity values were obtained. The nonsemicircular impedance plot characterizes a diffusion controlled interfacial charge transfer reaction. This feature was reproducible and evident at all temperatures.

The temperature dependence of the conductivity of this material is shown in Figure 5. The conductivity shows a linear temperature dependence between 20 and 60°C; however, nonlinear behavior above 60°C is quite evident and is believed to be related to the melting of the PEO:$LiBF_4$ complex. The room temperature conductivity of this material is 10^{-6} S cm^{-1}, significantly higher than the conductivity of the PEO:$LiBF_4$ polymer complex. It is now evident that the higher conductivity of Li_3N has begun to make a contribution to the composite electrolyte conductivity.

3. PEO:$LiBF_4$ - 40% Li_3N Material

This material was annealed at 125°C overnight before measuring its impedance. The temperature dependence of the conductivity of this material is shown in Figure 6 which shows the intersection of two linear regions at ~45°C. In the temperature region of 45-90°C, the conductivity varied from $5x10^{-5}$ to $5x10^{-4}$ S/cm, but the room temperature conductivity remained low, at $\cong 3x10^{-6}$ S cm^{-1}.

It was suspected that hand mixing of the batch materials in a mortar and pestle may not have produced a good homogeneous material; thus, the mixture of the above composition was micropulverized in a Brinkmann Model Retsch micropulverizer, and then the composite film was made using the previously described procedure. The temperature dependence of the conductivity of this material is presented in Figure 7. The conductivity data are very similar to those presented in Figure 6. These data add further credence to the reproducibility of the conductivity measurement.

Cyclic voltammograms of the Li/electrolyte/Li cell containing micropulverized Li_3N at 30.2°C are shown in Figures 8 and 9 at scan rates of 1 and 2 mV S^{-1}, respectively. In these two voltammograms, the anodic and cathodic peaks are well defined and symmetrical. The peak current densities are 13.8 and 16.92 μA cm^{-2} for 1 and 2 mV s^{-1} scan rates, respectively. Again, these voltammograms do not indicate any voltage instability of the electrolyte or secondary electrode reactions between the electrolyte and lithium. It may be further stated that such voltammograms at 30.2°C could not be obtained from PEO:$LiBF_4$ complexes due to their low ionic conductivities.

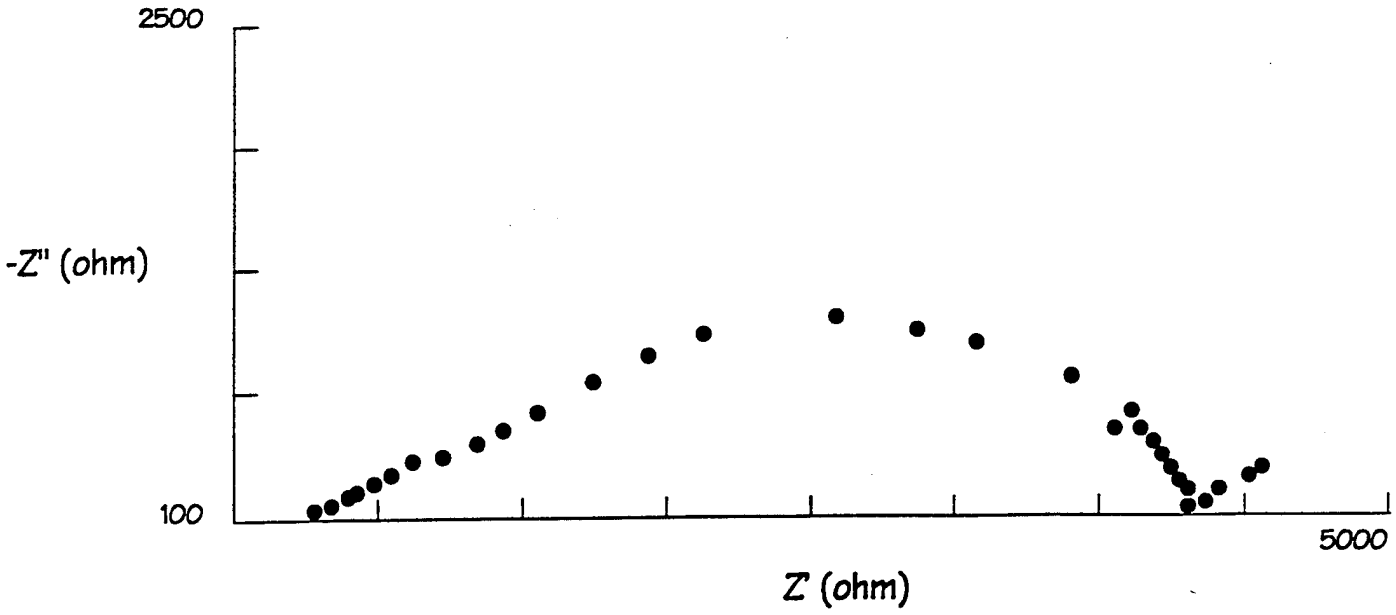

Figure 4. AC Impedance of a PEO:$LiBF_4$-25 wt% Li_3N Material at 90°C.

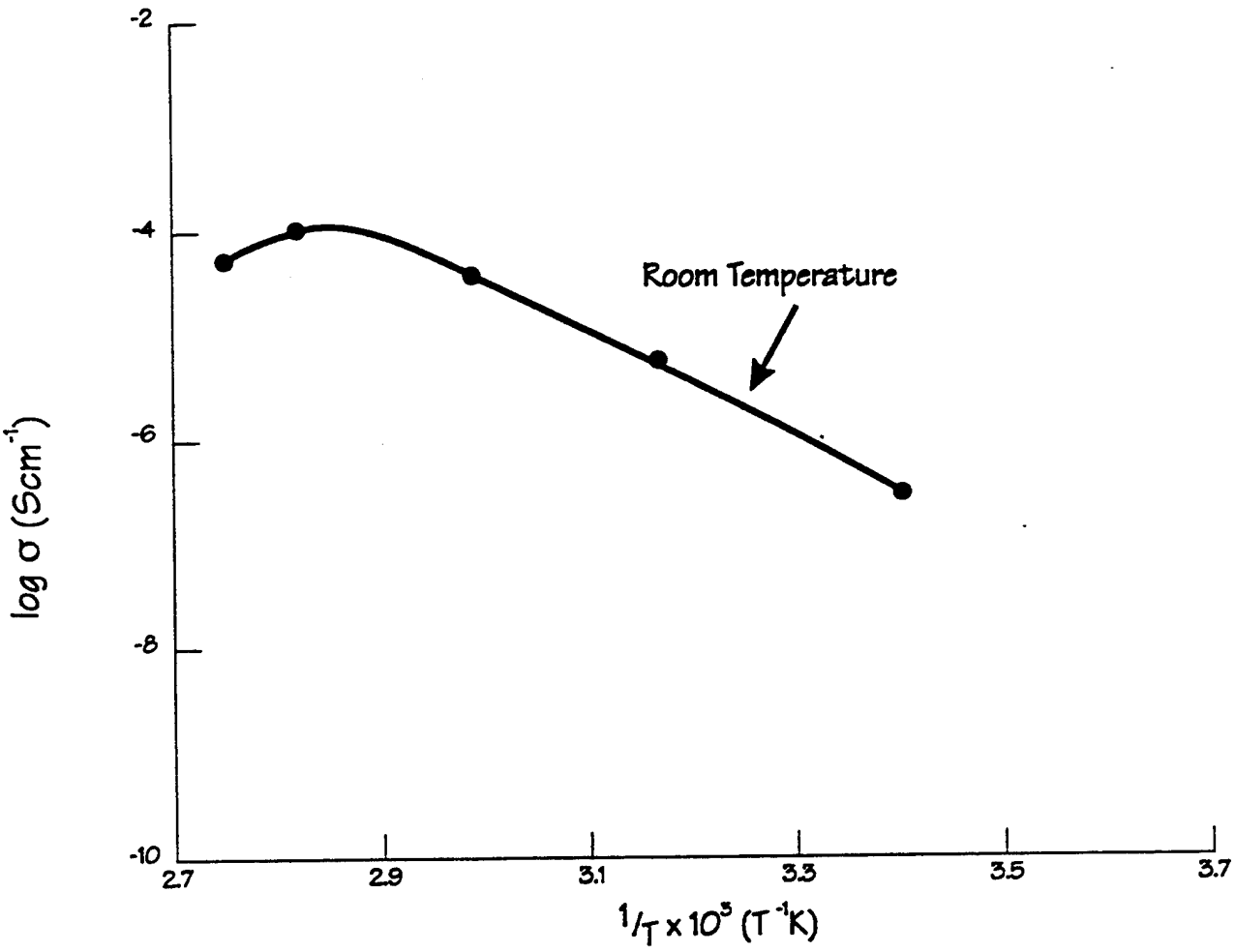

Figure 5. Temperature Dependence of Conductivity of PEO:$LiBF_4$-25 wt% Li_3N Solid Electrolyte Material.

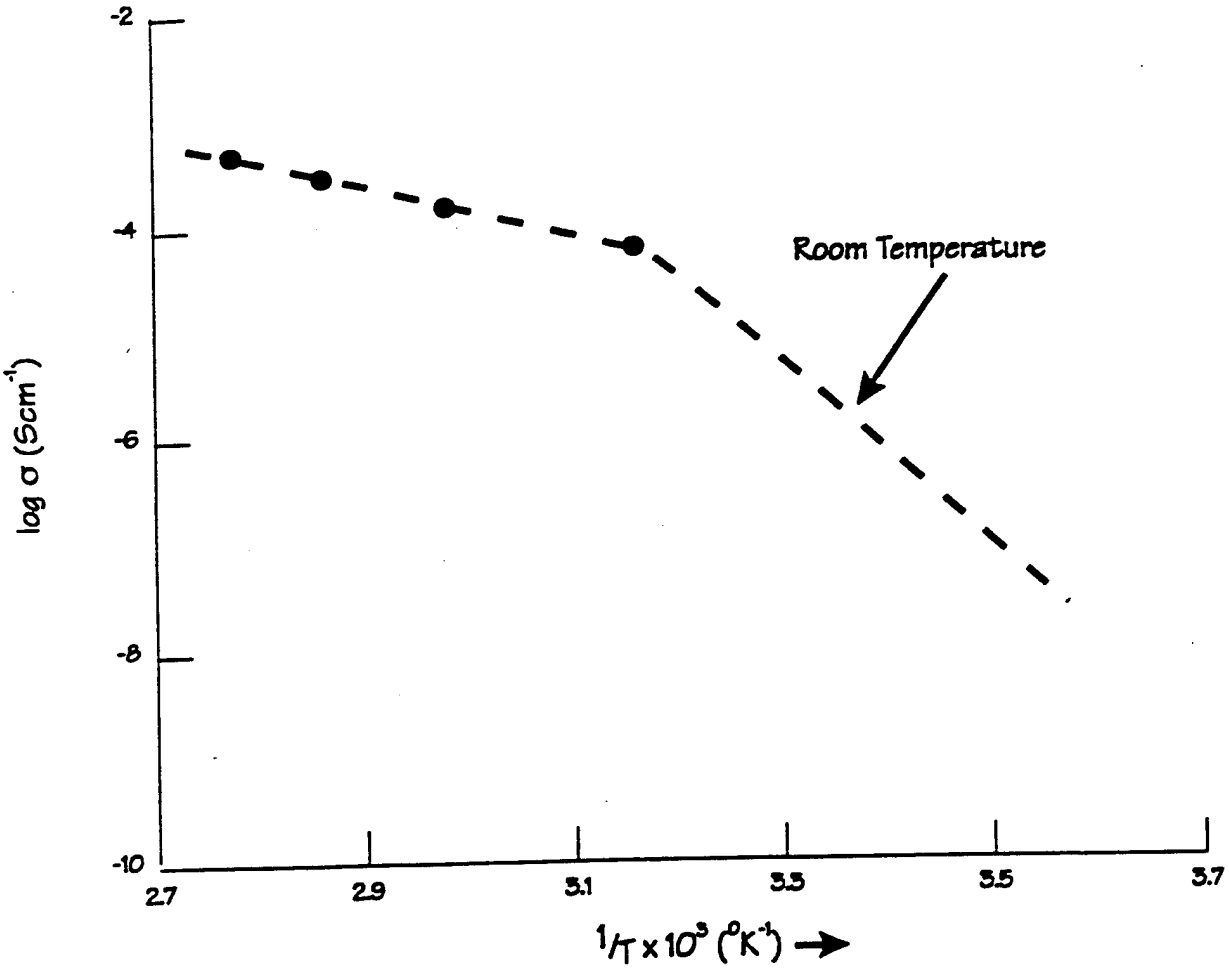

Figure 6. Log σ vs 1/T for PEO:$LiBF_4$-40 wt% Li_3N Annealed at 125°C Overnight.

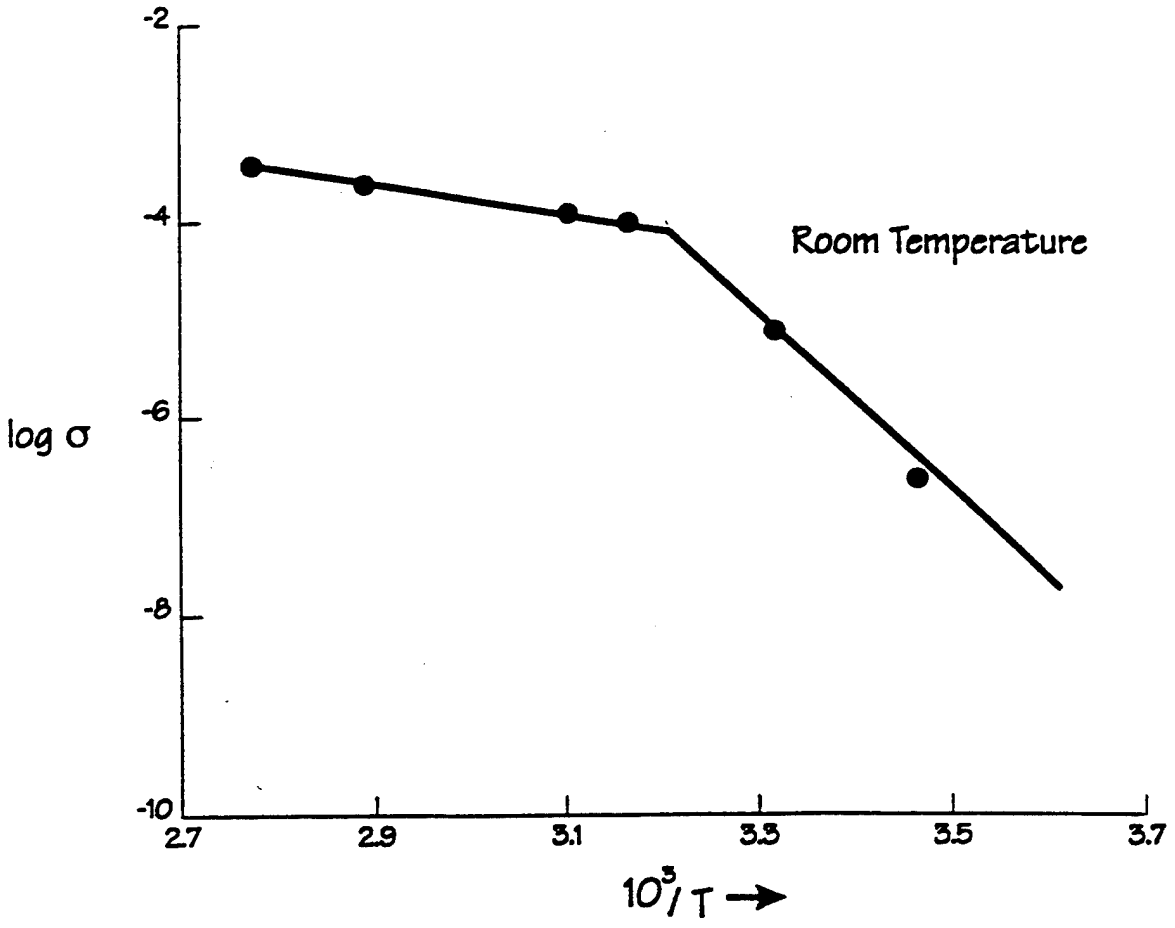

Figure 7. Log σ vs 1/T of PEO:$LiBF_4$-40 wt% Li_3N electrolyte. The batch materials were pulverized before making the film. The film was annealed at 125°C.

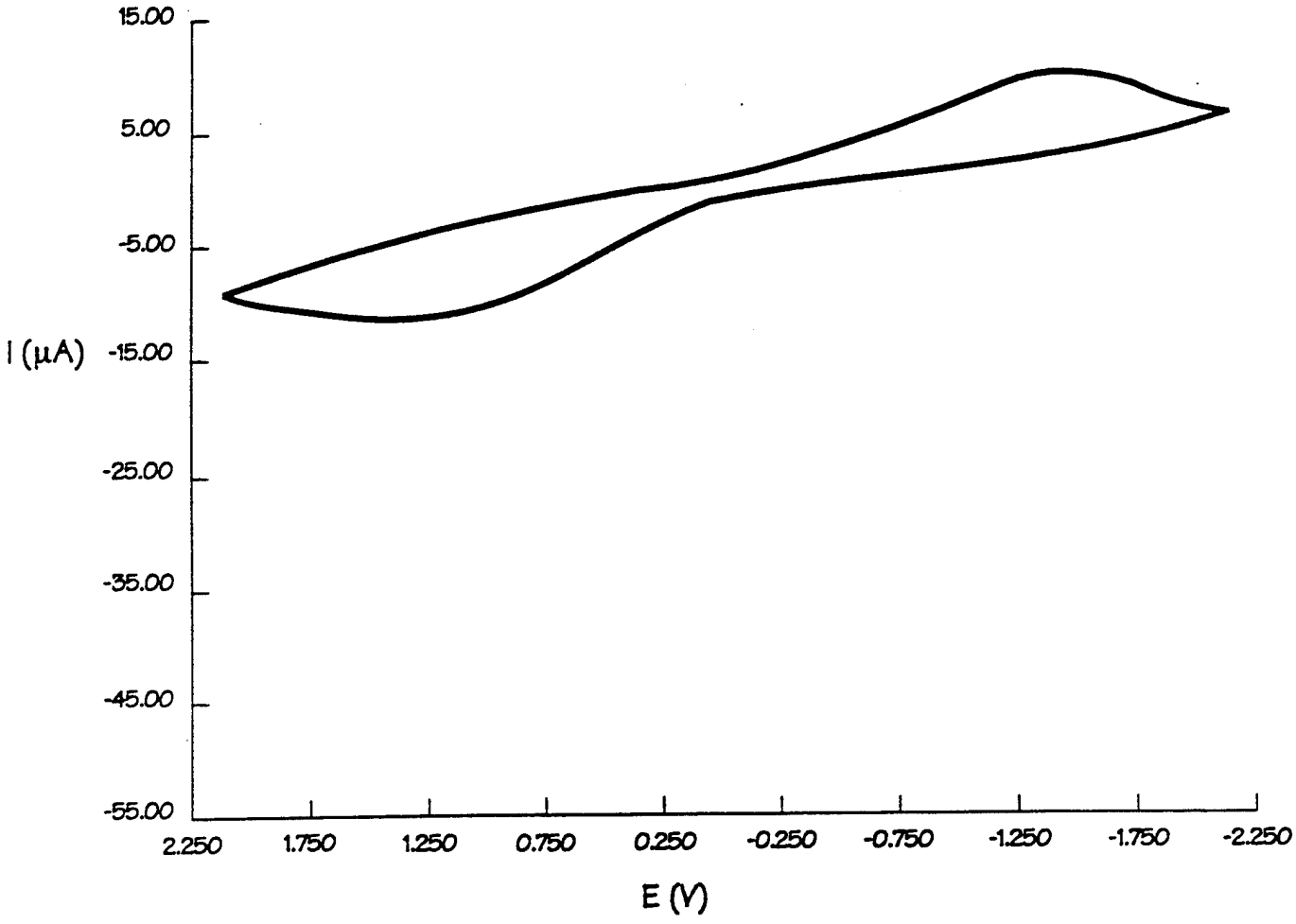

Figure 8. Cyclic Voltammogram of PEO:$LiBF_4$-40 wt% Li_3N Material at 30.2°C and a Scan Rate of 1 mVS^{-1}.

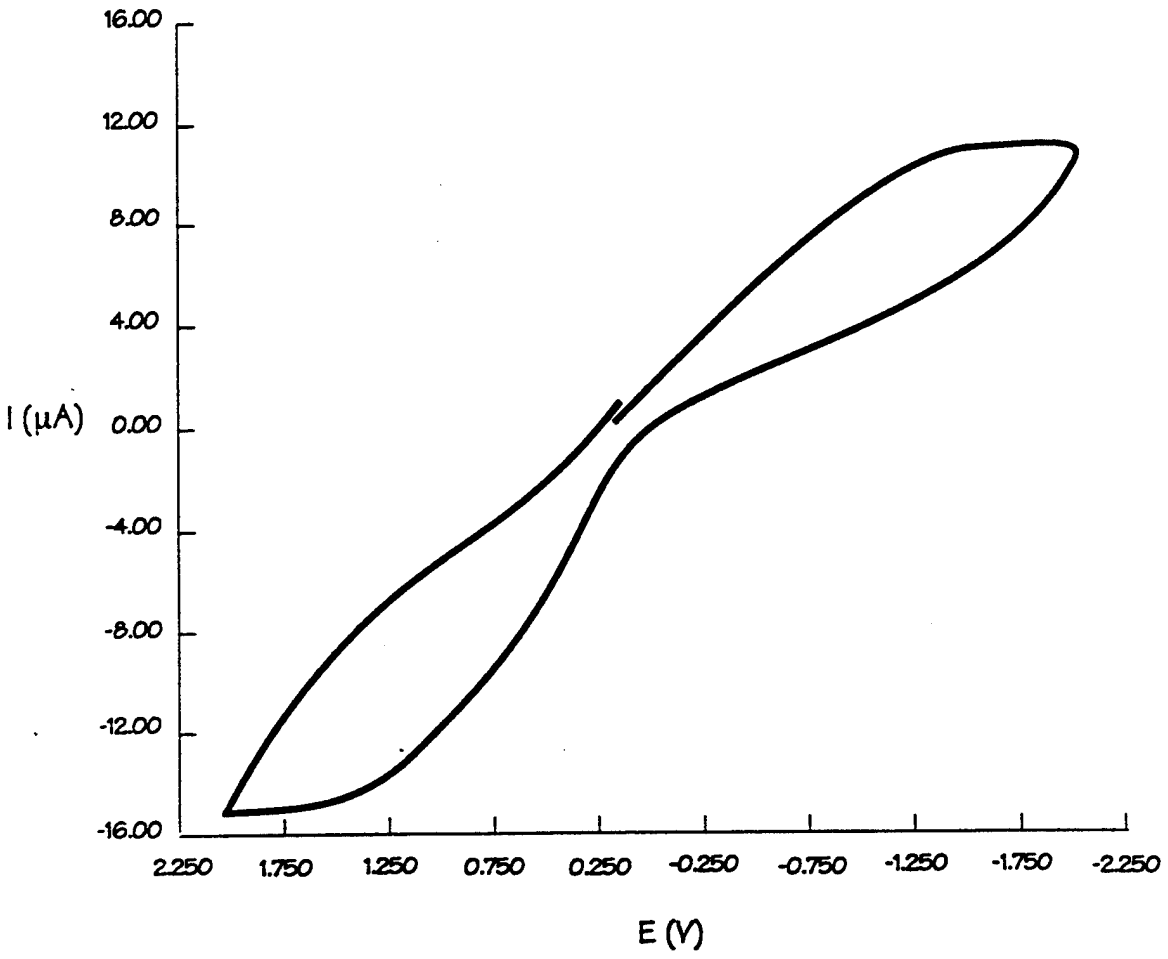

Figure 9. Cyclic Voltammogram of PEO:$LiBF_4$-40 wt% Li_3N Material at 30.2°C and a Scan Rate of 2 mVS^{-1}.

4. PEO:$LiBF_4$ - 50% Li_3N Material

The conductivity data for the material are shown in Figure 10. Although the high temperature (above ambient) conductivity remained unaffected, the low temperature (subambient) conductivity significantly increased. The ambient temperature conductivity of this material is about $5x10^{-6}$ S cm^{-1}. The slope of the conductivity curve around the ambient temperature decreased as compared to other materials, suggesting that the conduction mechanism has changed and the Li_3N is dominating the conductivity of the composite electrolyte.

5. PEO:$LiBF_4$- 60% Li_3N Material

Figure 11 shows the conductivity data of the 60% Li_3N material. As expected, the conductivity over the entire temperature range has increased, with the ambient temperature conductivity around $1.6x10^{-5}$ S cm^{-1}. A significant uncertainty developed in the conductivity determination at temperatures below the ambient temperature due to the not well-resolved ac impedance spectrum. A typical ac impedance plot at 15°C is shown in Figure 12. It should be noted that the z' intercept used to calculate bulk resistivity is not easily discernible.

A cyclic voltammogram of a Li/composite/Li cell at 25°C and with a 2 mV S^{-1} sweep rate is shown in Figure 13. The voltammogram is quite symmetric and again reveals the absence of any secondary peaks.

6. PEO:$LiBF_4$ - 70% Li_3N Material

Attempts were made to prepare films containing the 70 wt% Li_3N. These films were brittle and difficult to handle. The data obtained from the ac impedance measurements were inconclusive and thus no further attempts were made to synthesize and characterize composite materials over 60% Li_3N.

3.2 Effect of Annealing

In previous measurements some influence of annealing on conductivity was observed. Subsequently, it was realized that annealing has a major influence on conductivity and thus the effect of it was further pursued and this section presents some of the distinguishing features of annealed specimens.

Table 2 provides conductivity data of 25% Li_3N material annealed at various temperatures. It should be noted that annealing at 100°C increased the conductivity substantially, whereas further annealing at 125°C had little effect on conductivity.

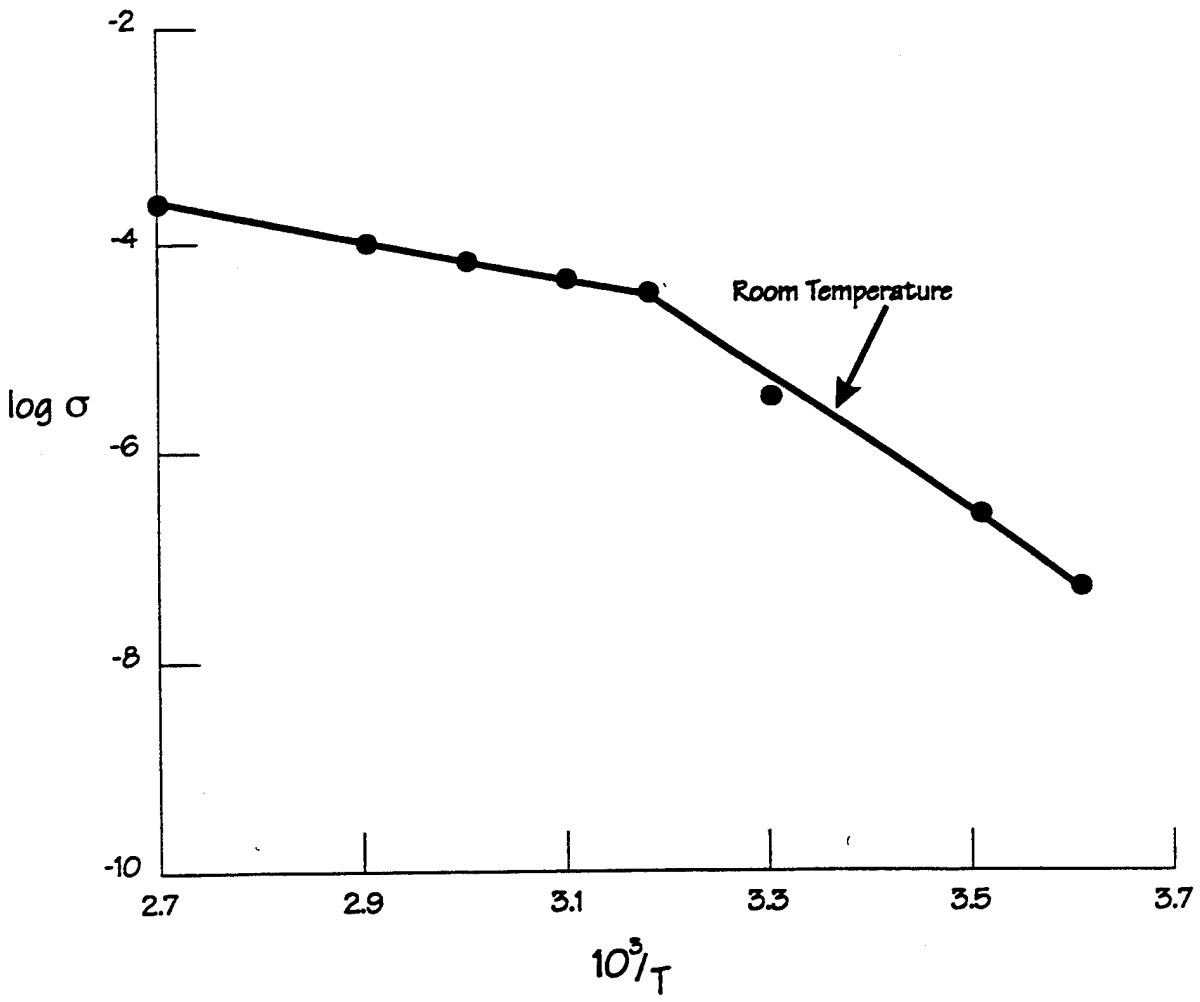

Figure 10. Log σ vs 1/T for PEO:$LiBF_4$-50 wt% Li_3N Material Annealed at 100°C for 48 hours.

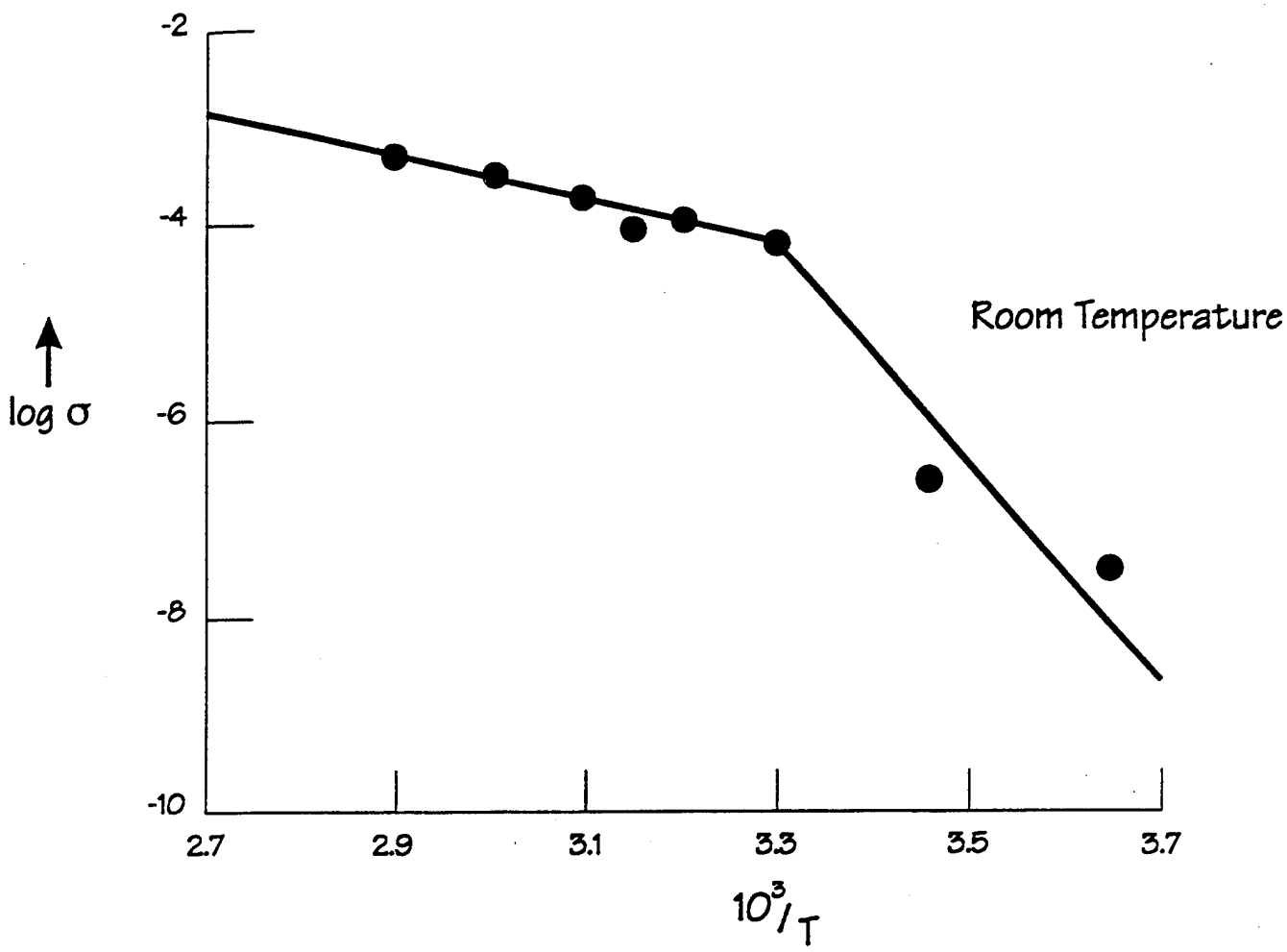

Figure 11. Log σ vs 1/T of PEO:$LiBF_4$-60 wt% Li_3N Composite Electrolyte Annealed at 125°C.

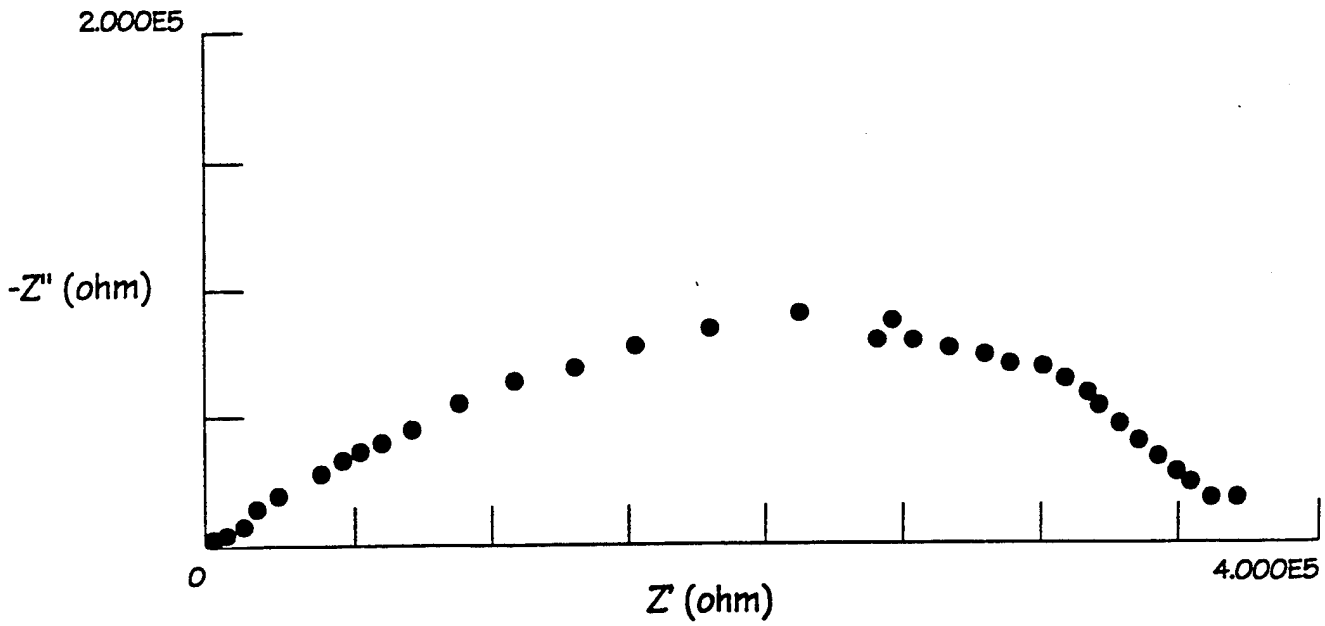

Figure 12. AC Impedance Spectrum of PEO:$LiBF_4$-60 wt% Li_3N Composite Electrolyte at 15°C.

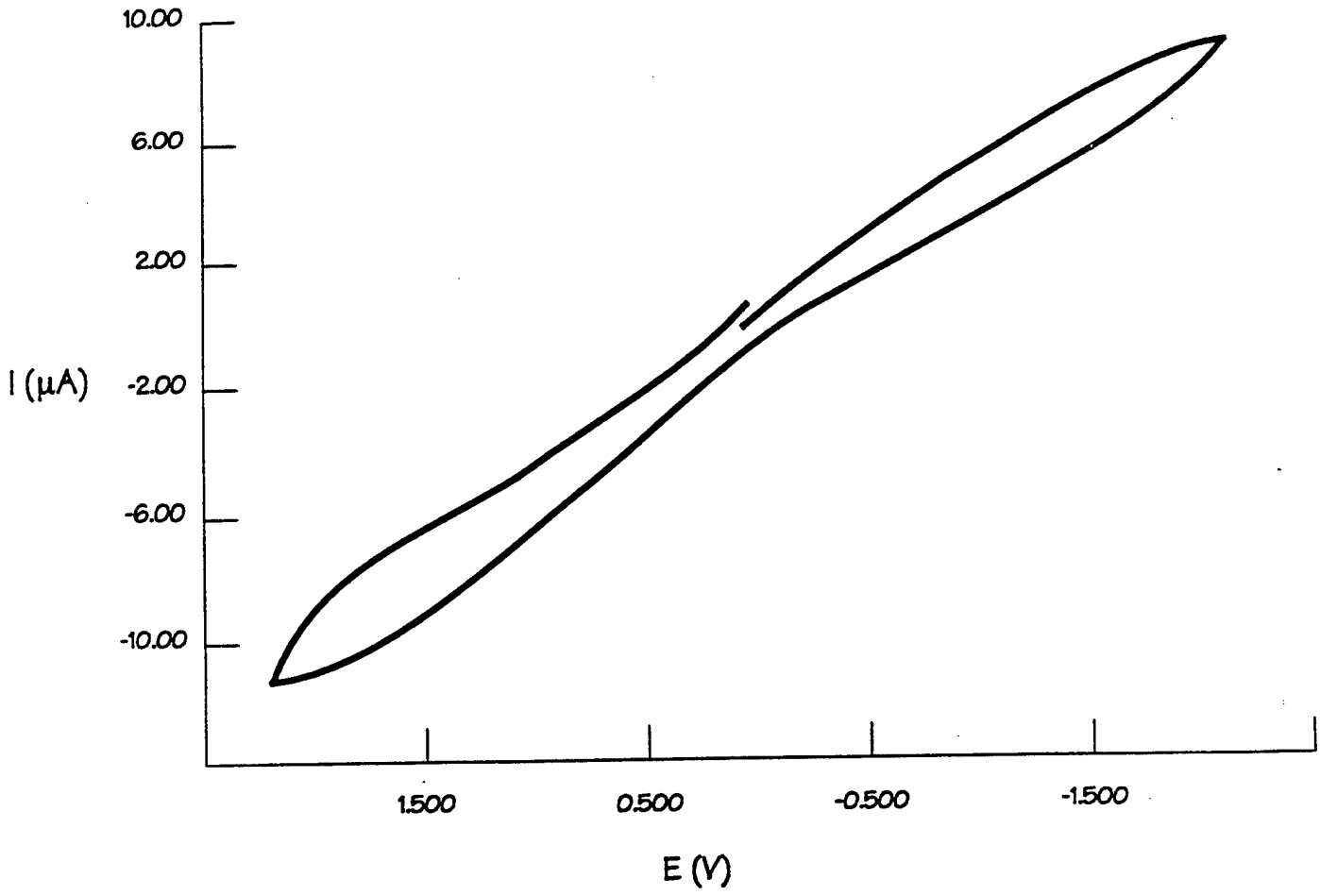

Figure 13. Cyclic Voltammogram of the Li/Composite/Li Cell (Li_3N=60%) at 25°C and Sweep Rate of 2 mVS^{-1}.

TABLE 2

Temperature Dependence of Conductivity (σ) of PEO:$LiBF_4$-25 wt% Li_3N Composite Electrolytes Annealed at Various Temperatures and Times

Temperature (°C)	A Annealed at 60°C for 12 hrs	B A + 100°C for 2 hrs	C B + 125°C for 12 hrs
0	2.14×10^{-10}	---	---
15	4.36×10^{-9}	---	
20			3.57×10^{-7}
30	5.97×10^{-8}	---	
40			7.8×10^{-6}
45	7.52×10^{-7}	---	
60	1.5×10^{-5}	8.72×10^{-5}	5.88×10^{-5}
75	---	2.40×10^{-4}	---
80			1.26×10^{-4}
90	---	4.76×10^{-4}	9.17×10^{-5}

Figure 14 shows conductivity data of 60% Li_3N material annealed at 90°C for 24 hours and then the same specimen further annealed at 125°C for 24 hours. There is a slight decrease in the high temperature (50-90°C) conductivity, while the low temperature conductivity exhibited a remarkable increase due to further annealing at 125°C. It should also be noted that the temperature dependence of conductivity over the entire range (0-90°C) decreased significantly. The activation energy calculated from the temperature dependence data was found to be around 5 kcal mol^{-1} which is even lower than the activation energy for lithium ion conduction in Li_3N ($\perp C$ = 6.7 kcal mol^{-1}, $||$ C = 11.30 kcal mol^{-1}).

Figure 15 again shows conductivity data of a 60% Li_3N specimen annealed at 125°C overnight and then additionally annealed at 125°C (overnight) and 135°C (overnight). The first annealing yields typical conductivity values, i.e., high conductivity at higher temperatures and steep temperature dependent conductivity at lower temperatures. Additional annealings at 125°C and 135°C alter the low temperature segment of the curve in a remarkable manner which is consistent with the data of Figure 14. Quite noticeable in this figure is a knee around the 40-70°C range in the conductivity curve of the over-annealed specimen. The knee corresponds to the melting region of PEO and reflects the transition from a molten state to a solid state. The activation energy calculated from the linear regions of the curve of the overannealed specimen is approximately 5 kcal mol^{-1}.

Figure 16 presents conductivity data of a 60% Li_3N specimen first annealed at 145°C for 24 hrs and then additionally annealed at 145°C for 72 hrs. Again this figure illustrates similar features as shown in Figures 14 and 15.

The reproducibility of conductivity enhancement due to annealing in the 90-145°C temperature region is extremely good. The annealing temperature and time can be precisely determined to optimize the conductivity, however, it has not been done in this work due to resource constraints. The parameters that we considered in selecting annealing conditions were melting points of PEO (68°C) and Li (180°C), volume fraction of Li_3N, and thickness of the electrolyte film. Slight improvements in conductivity are achieved by annealing the specimen in the 90-125°C region for shorter periods of time (<50 hrs). Major improvements in conductivity occur by annealing for longer periods of time (>50 hrs) in the 90-125°C region or at higher annealing temperatures (>125°C) for shorter times (<50 hrs). It is obvious that 145°C may not be the upper limit; perhaps one can go up to 170°C and reduce the annealing time to a few hours.

Having examined the experimental data on the effect of annealing, the obvious question arises, i.e., why does annealing at higher temperatures and prolonged time enhance conductivity? Perhaps one could propose that the annealing leads to the formation of a phase in the electrolyte

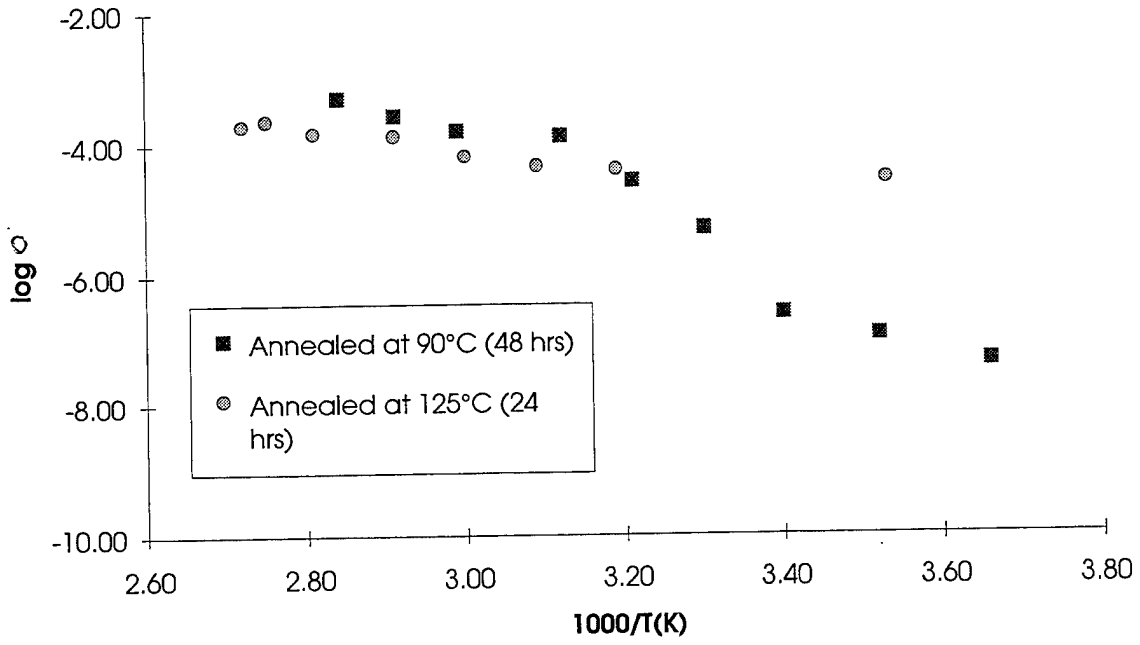

Figure 14. Conductivity of PEO:$LiBF_4$-60 wt% Li_3N Material Annealed at 90°C and 125°C.

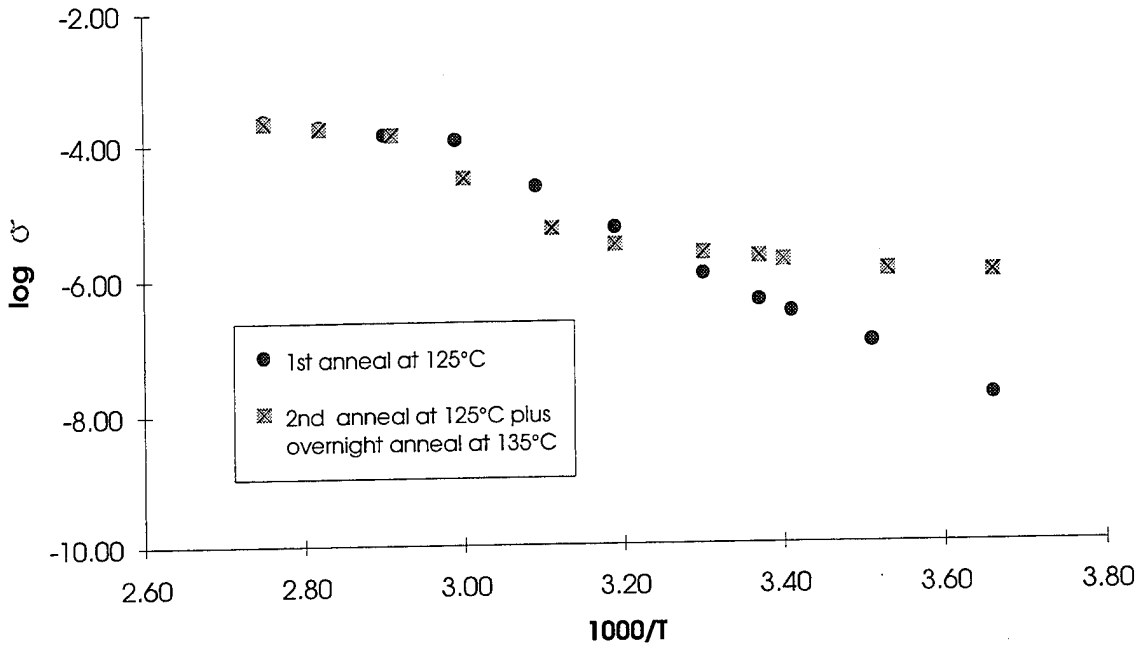

Figure 15. Conductivity Data of PEO:$LiBF_4$-60% Li_3N Material Annealed at 125°C and Then Additionally Annealed at 125°C and 135°C.

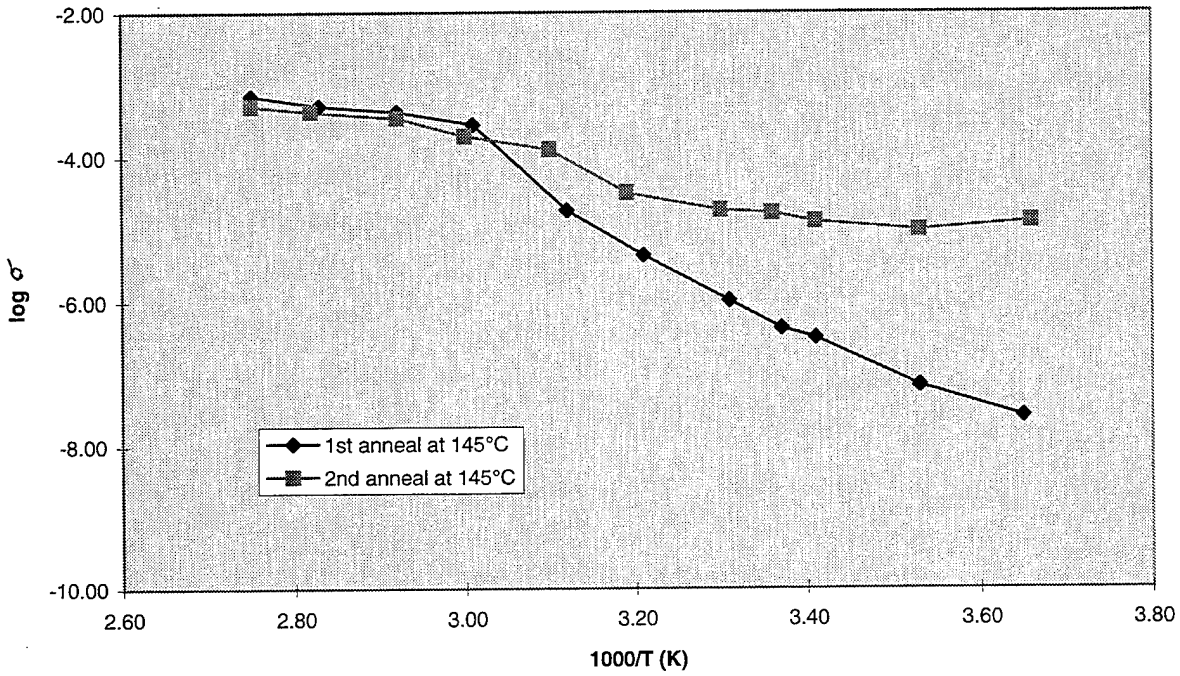

Figure 16. Conductivity Data of PEO:$LiBF_4$-60% Li_3N Material Annealed at 24 hrs and 72 hrs, respectively.

which enhances the conduction process. Based on this proposal, we conducted differential scanning calorimetry (DSC), thermogravimetric analysis (TGA), and x-ray diffraction studies on some of these annealed specimens and these data are presented in subsequent sections. In all these studies, 60% Li_3N material was used and the specimens consisted of (a) as-prepared, (b) annealed at 90°C for 24 hrs under helium atmosphere, (c) annealed at 145°C for 24 hrs under helium atmosphere.

3.3 Thermogravimetric Analysis (TGA)

Figures 17 through 19 show TG/DTG curves for specimens (a), (b), and (c). The as-prepared specimen, Figure 17, exhibits three peaks located around 62, 111, and 339°C. The 62°C peak is believed to be related to decomposition of $LiBF_4$ and loss of fluorine. The 111°C peak may be attributed to the loss of moisture, and the 339°C peak may be related to decomposition of PEO. It should be noted that only 12.69% PEO is decomposed. The composite mixture contains 30% PEO, 10% $LiBF_4$, and 60% Li_3N. It is interesting to note that specimen (a) gains substantial weight as the temperature is increased over 350°C. The specimen may have picked up nitrogen from the atmosphere or reacted with the container. Specimen (b) (Figure 18) shows much stable behavior at lower temperatures. Apparently annealing at 90°C stabilized the material. The losses up to about 300°C account for only 1.841% of the material as compared to 5.267% for the as-prepared specimen. The peak corresponding to PEO decomposition around 329°C and weight gain beyond this temperature remain similar to Figure 17. A low temperature peak around 54°C reappears in specimen (c) (Figure 19) and the low temperature weight loss increases to 2.956%. The PEO decomposition temperature shifts to a lower temperature; however, the degree the PEO decomposition and weight gain above this temperature are significantly reduced.

The TGA data point out two important events: annealing stabilizes the material through complex chemical reactions including decomposition of $LiBF_4$ at 62°C and during processing of the material, approximately 20% PEO is converted to some other phase which is not decomposable up to about 600°C. The explanation for weight gain in the 350-600°C region remains uncertain at present. Further experiments will have to be conducted to understand this phenomenon.

3.4 Differential Scanning Calorimetry (DSC)

Figure 20 shows DSC data obtained from specimen (a). The figure shows one endothermic peak located around 62°C and two exothermic peaks located at 137.69 and 343.85°C, respectively. The endothermic peak is attributed to the complexation of PEO with $LiBF_4$ and also corresponds to the TGA peak (Figure 17). The two exothermic peaks may be

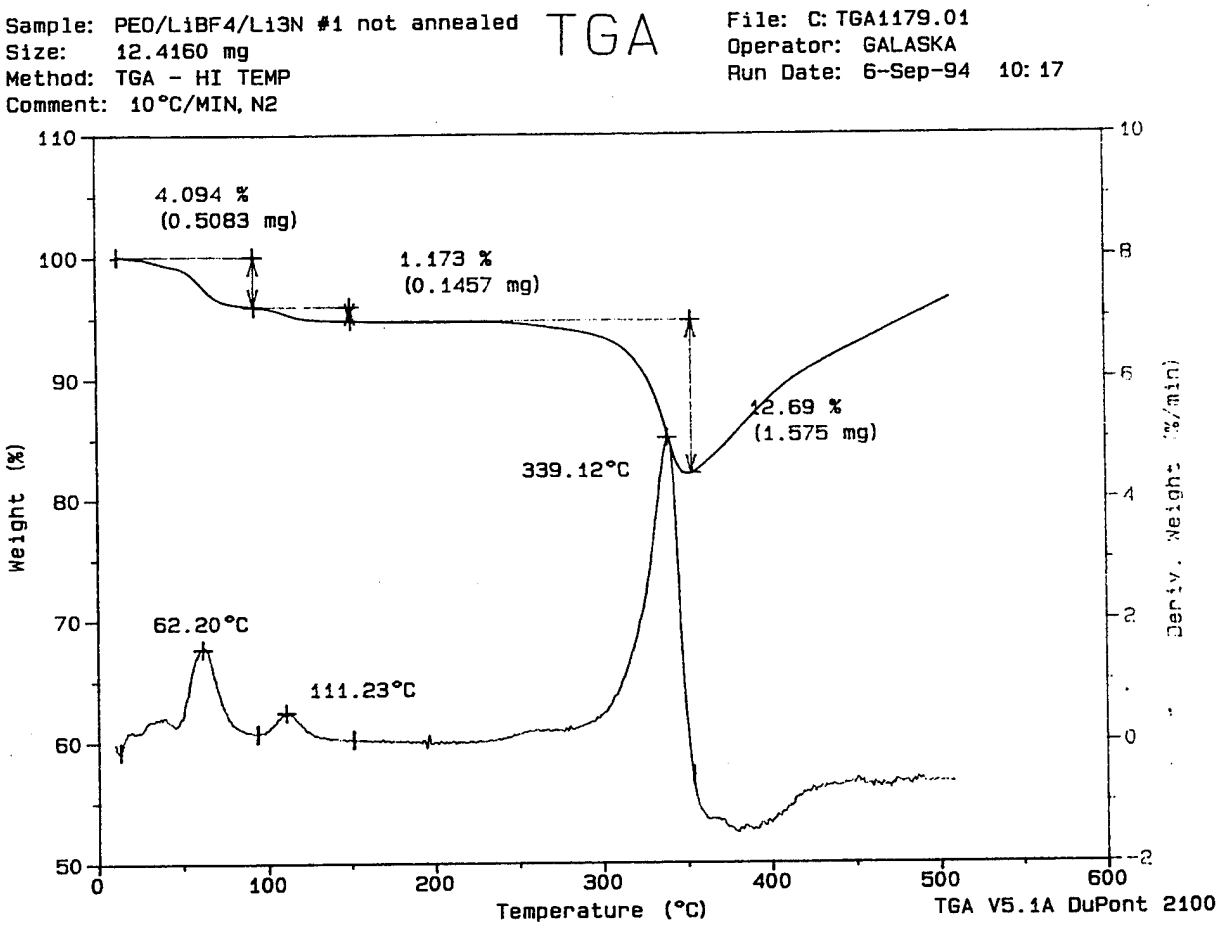

Figure 17. TGA Curve of As-Prepared PEO-$LiBF_4$-60 wt% Li_3N Specimen (a).

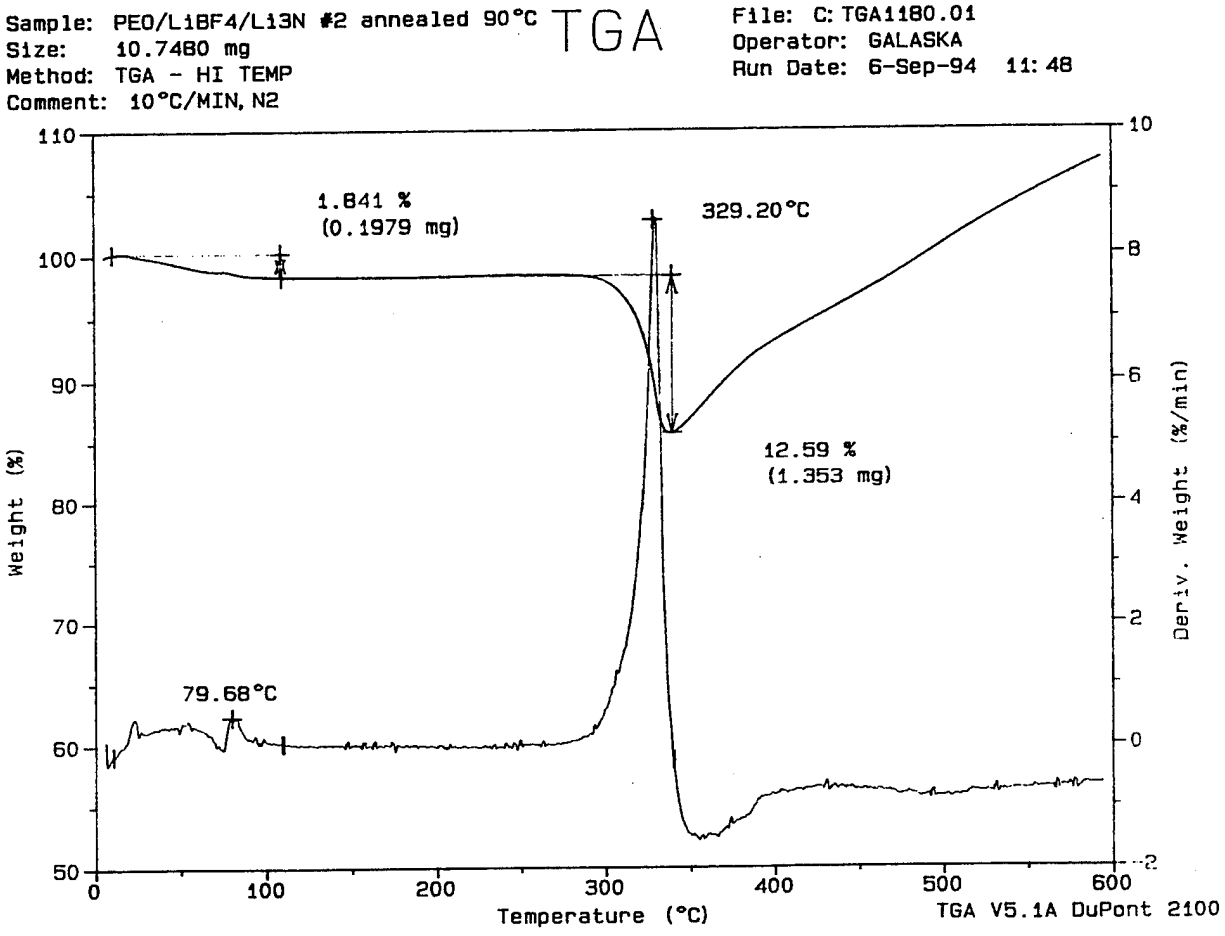

Figure 18. TGA Curve of PEO:$LiBF_4$-Li_3N Specimen (b) - Annealed at 90°C.

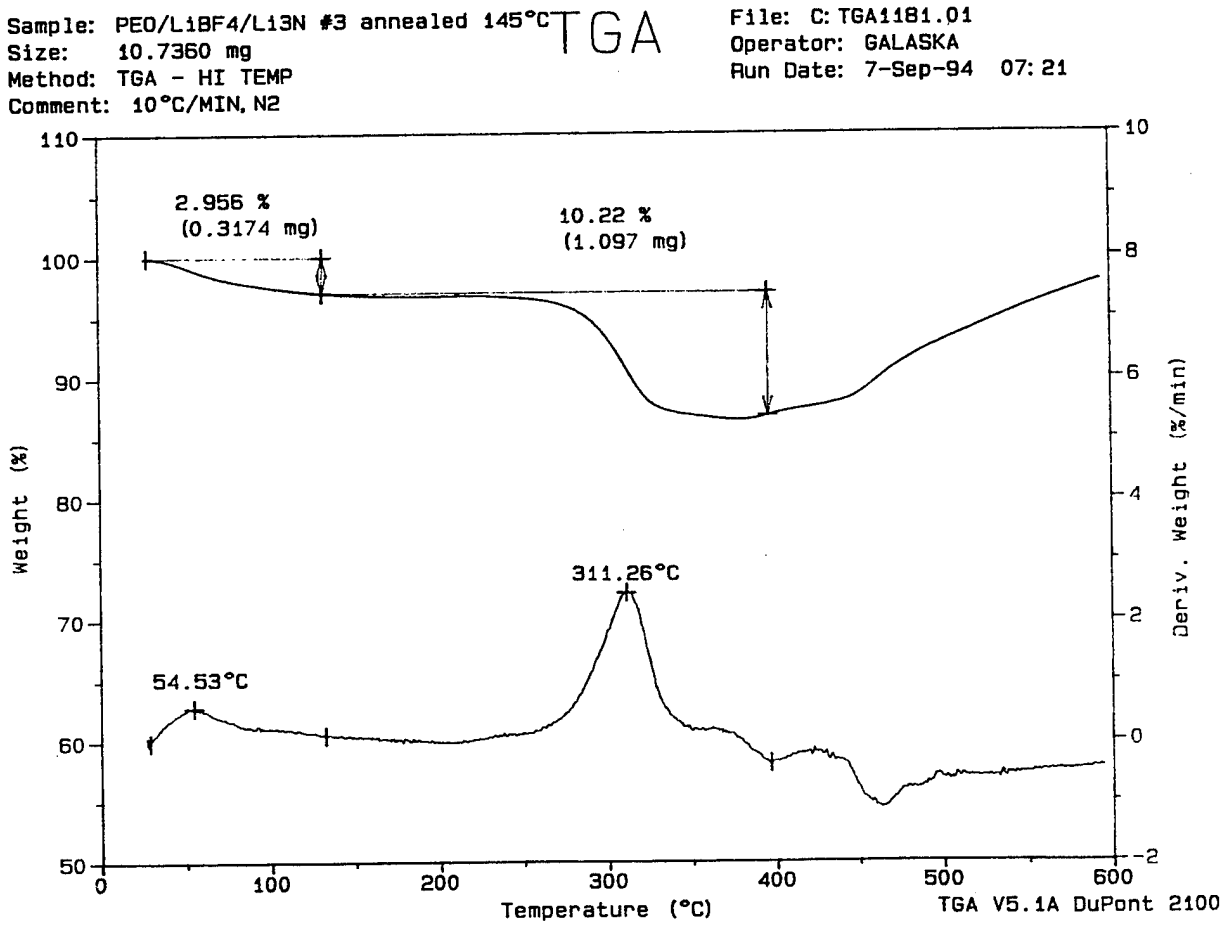

Figure 19. TGA Curve of PEO:$LiBF_4$-60 wt% Li_3N Specimen (c) - Annealed at 145°C.

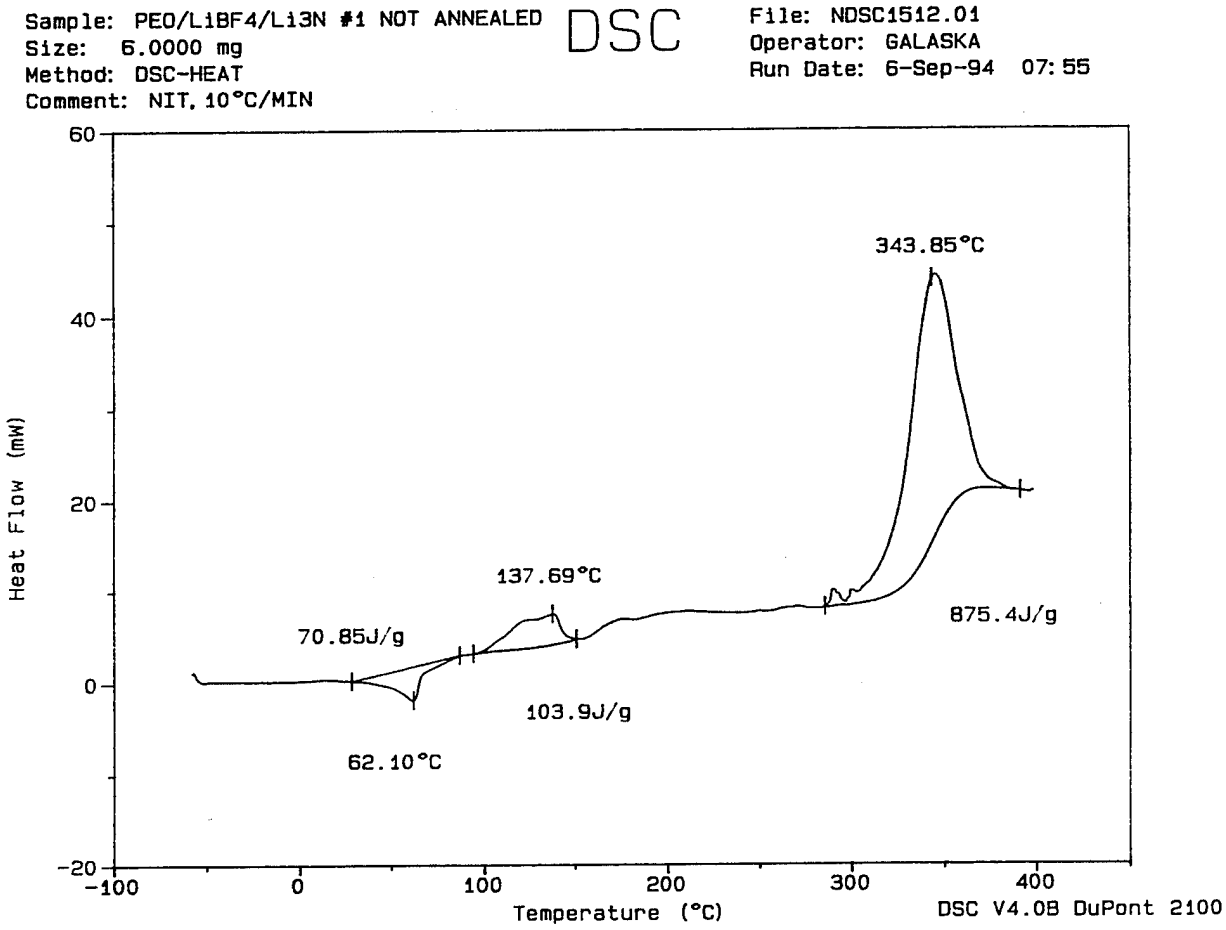

Figure 20. DSC Data of PEO:$LiBF_4$-60 wt% Li_3N Specimen (a) - As-Prepared.

attributed to phases formed due to interactions between PEO, $LiBF_4$, and Li_3N. The DSC curve for specimen (b) which was annealed at 90°C (Figure 21) shows a reduction in the intensity of the endothermic peak at 54.70°C. The exothermic peak at 137°C merges with a much broader exotherm extending from 100 to 200°C. This exotherm reveals at least four peaks, and perhaps it is of significant interest to explain new phase formation in the high conductivity materials. The highest exotherm peak at 345.60°C shifts slightly toward a higher temperature in comparison to the as-prepared specimen. Annealing the specimen at 145°C for 24 hrs eliminates the low temperature endotherm (Figure 22), whereas the intermediate temperature exothermic peak is broader and shows a single peak centered around 288°C. The highest temperature exotherm has further shifted to an even higher temperature, 357°C.

It is now apparent from the TGA and DSC data that the processing of the composite electrolyte material followed by annealing heat treatments leads to the formation of a new phase or phases in which part of PEO and the entire $LiBF_4$ are consumed. A reaction of the type represented by (A) is conceivable and thus the processing technique yields

$$[(\text{-O-CH}_2\text{-CH}_2\text{-})_3 + Li_3N]_n \rightarrow \left[\text{Li-O-CH}_2\text{CH}_2\text{-N} \begin{matrix} \text{CH}_2\text{-CH}_2\text{-O-Li} \\ \text{CH}_2\text{-CH}_2\text{-O-Li} \end{matrix}\right]_n \qquad \text{(A)}$$

a new type of material, in which it is believed that $LiBF_4$ initiates the reaction.

3.5 X-ray Diffraction

The x-ray diffraction patterns of three specimens as-prepared, annealed at 90°C, and annealed at 145°C are shown in Figure 23a-1c, respectively. The Li_3N remains a major crystalline phase in the electrolyte in all three specimens. A slight shift in the peak locations and sharpening occur as the annealing temperature is increased. Table 3 shows tabulated d-spacings and corresponding crystalline phases. The $LiBF_4$ phase is absent in specimen (c). There are several low intensity peaks which were not identified and indexed. Perhaps these are the peaks from the new phase and these are moderately strong in specimen (c). The sharpening of Li_3N peaks implies that either the grains have become larger or smaller grains have reacted with PEO forming a new phase and only larger grains are left.

3.6 Infrared Spectroscopy

Table 4 shows infrared absorption bands of 60% Li_3N electrolyte material heat treated at 145°C, along with the bands of component materials Li_3N, $LiBF_4$, PEO, and PEO:$LiBF_4$. The composite electrolyte exhibits characteristic absorption bands located around 3675, 2725, 1618, and 1113 cm^{-1}. Stretching vibration of the N=0 group usually exhibits a strong band located around 1600 cm^{-1} and perhaps 1618 cm^{-1} could be assigned to it. The other bands at 3675,

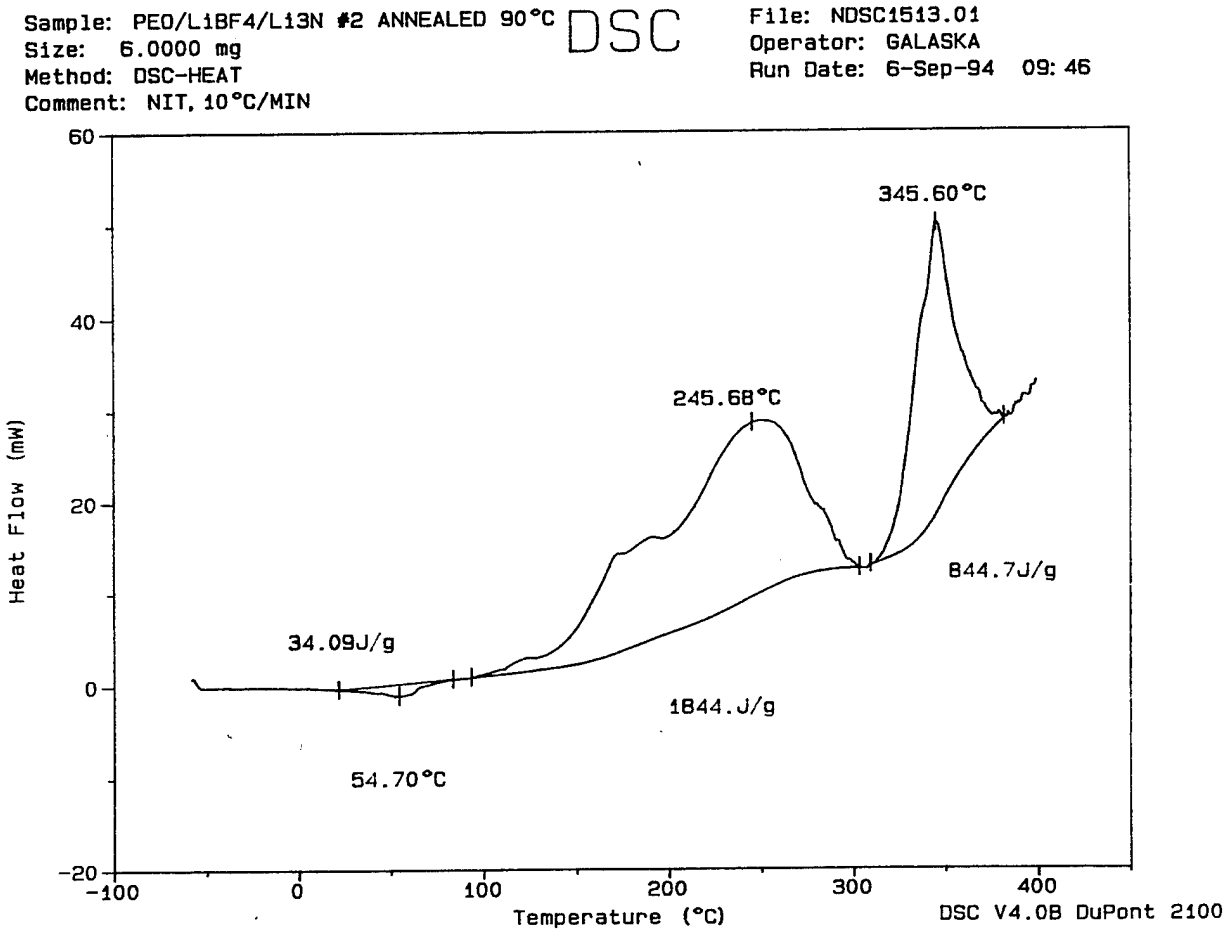

Figure 21. DSC Curve of PEO:$LiBF_4$-60 wt% Li_3N Specimen (b) - Annealed at 90°C for 24 hrs.

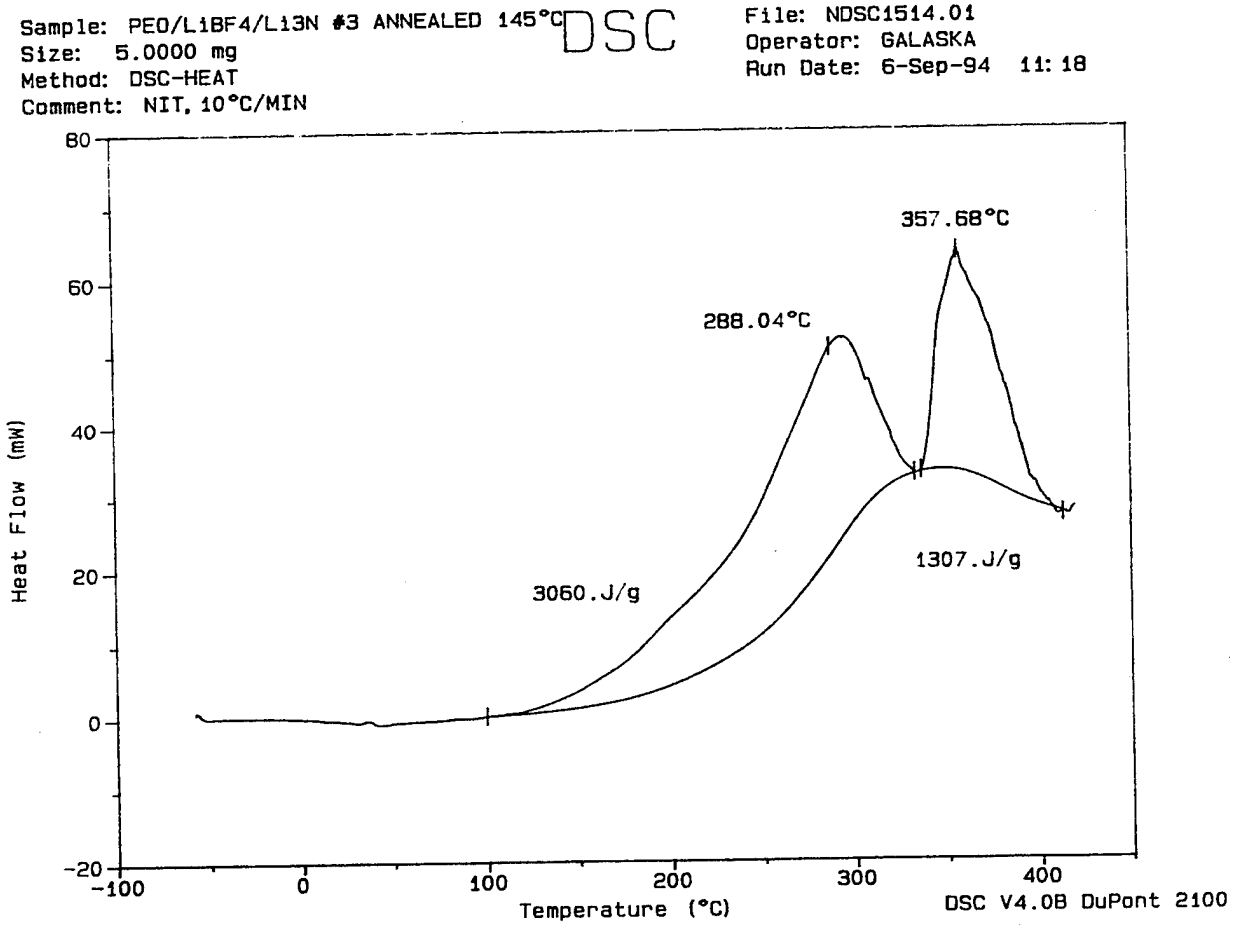

Figure 22. DSC Curve of PEO:$LiBF_4$-60 wt% Li_3N Specimen (c) Annealed at 145°C for 24 hrs.

Figure 23. X-ray Diffraction Patterns of (a) PEO:$LiBF_4$-60 wt% Li_3N as-prepared, (b) PEO:$LiBF_4$-60 wt% Li_3N - annealed at 90°C for 24 hrs, and (c) PEO:$LiBF_4$-60 wt% Li_3N - annealed at 145°C for 24 hrs.

TABLE 3

d-spacings of PEO-60 wt% Li_3N Composite Specimens

Specimen (a) as prepared			Specimen (b) annealed at 90°C for 24 hours				Specimen (c) annealed at 145°C for 24 hours		
2θ	I	d	2θ	I	d	2θ	I	d	
22.75	100	3.909	22.75	100	3.909	23.00	100	3.867	Li_3N
25.95	3	3.433	25.95	3	3.433				
26.75	3	3.333	26.75	3	3.333				$LiBF_4$
28.00	25	3.187	28.00	25	3.187	28.25	42	3.159	Li_3N
30.30	6	2.950	30.30	5	2.950	30.50	26	2.931	
32.85	3	2.726	32.85	3	2.726	32.35	11	2.767	
33.20	1	2.698	33.15	2	2.702	33.50	4	2.675	
35.85	9	2.505	35.85	9	2.505	35.85	4	2.505	
38.40	5	2.344	38.40	5	2.344	38.65	14	2.329	
44.90	4	2.019	44.90	4	2.019	44.85	16	2.021	
46.70	6	1.945	46.70	6	1.945	46.90	14	1.937	Li_3N
49.75	8	1.833	49.75	8	1.833	50.00	14	1.824	Li_3N
50.95	3	1.792	50.95	3	1.792	51.05	2	1.789	
55.45	7	1.657	55.45	7	1.657	55.65	13	1.652	Li_3N

TABLE 4

IR Absorption Bands in Li_3N, $LiBF_4$, PEO, PEO:$LiBF_4$, and 60% Li_3N Material Heat Treated at 145°C

Frequency	$LiBF_4$	PEO	PEO:$LiBF_4$ (O:Li=8)	60% Li_3N Heat Treated at 145°C
				3675
		2943	2942	
			2922	
		2885	2886	
		2860	2862	
				2725
2361				
2338				
	1636			1618
		1465	1464	
				1345
		1341	1341	
		1279	1279	1281
1257				
		1238	1240	1243
		1145	1147	1147
				1113
		1105	1108	
		1058	1058	
	1052			
			995	
			964	
		959		
		841	839	
	639			
	533			

2725, and 1113 remain unassigned and a thorough investigation is required to assign these bands to specific vibrations of molecular groups. Nonetheless, formation of a new phase and chemical bonds is further corroborated by the absorption data.

3.7 Effect of Li_3N Particle Size

In solid polymer-ceramic composite electrolyte literature, sporadic reports have been made that the particle size of the ceramic phase may have a significant influence on the conductivity of the electrolyte. With this background, PEO-Li_3N composite electrolytes containing 40 and 60 wt% Li_3N were formulated. Only two particle sizes with their distribution peaks located around 25 and 100 μm were used. The specimen in a symmetric cell (Li/electrolyte/Li) configuration was annealed at 90°C overnight. The temperature dependence of conductivity for 40% Li_3N material is shown in Figure 24. The two curves corresponding to particle sizes of 25 and 100 μm virtually overlap each other. The curves show two regions: the high temperature region (50-90°C) is characterized by high conductivity ($\log \sigma \cong 3.5$) and low activation energy for the conduction, whereas the low temperature region (0-50°C) signifies a high activation energy leading to pronounced reduction in conductivity as the temperature is lowered. The low temperature region also corresponds to formation of crystalline regions in the electrolyte.

The temperature dependence of conductivity for 60% Li_3N material is shown in Figure 25. In this case the larger particle size material yields a slightly higher conductivity, particularly in the low temperature region. Again, the conductivity curves are comprised of two segments similar to Figure 24.

The data presented in Figures 24 and 25 clearly demonstrate that the finer particles provide little benefit with regard to conductivity. In fact, coarser particles augment conductivity at lower temperatures. This is consistent with the earlier report by Skaarup et al.[8] on $Li3N_4$ containing solid electrolyte materials.

3.8 Effect of Li_3N on Conductivity of the Composite Electrolyte

It is now recognized that two distinctly different factors govern the conductivity of PEO-Li_3N composite electrolyte. The first factor results from intrinsically high conductivity of Li_3N material and lower degree of annealing. The second factor originates from the formation of a new phase due to annealing at higher temperatures or longer times. The second factor contributes to a pronounced increase in the low temperature conductivity. The effects of these two factors can easily be distinguished from the examination of the conductivity data.

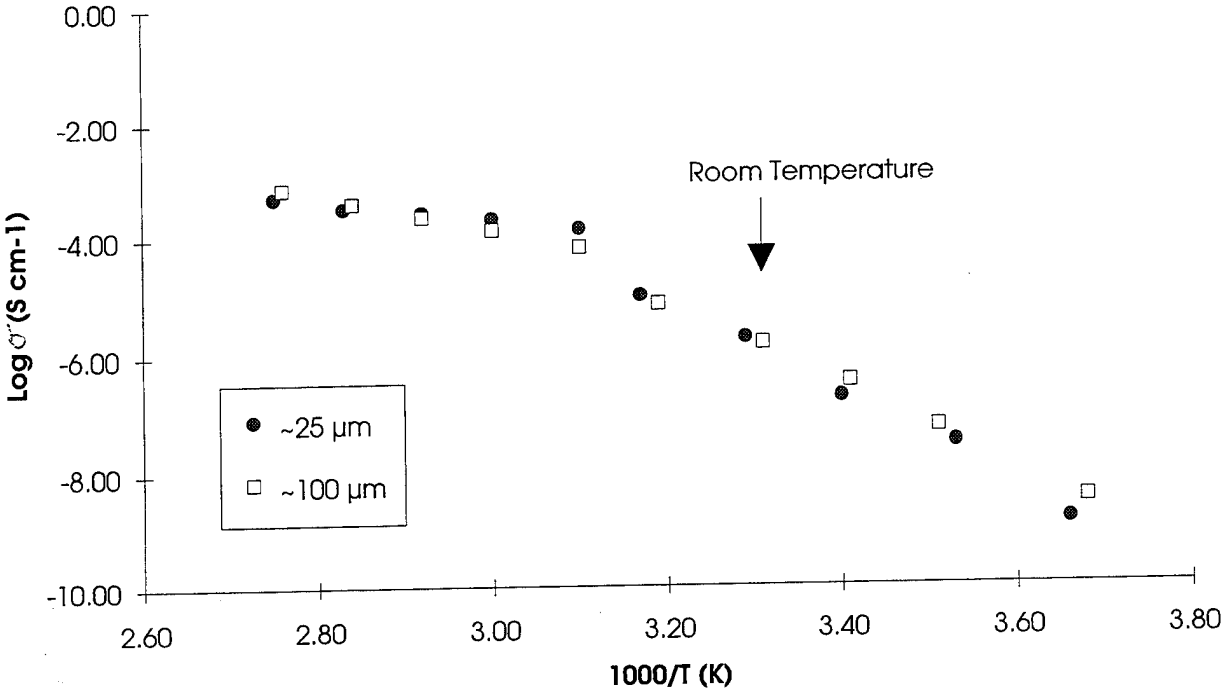

Figure 24. Effect of Particle Size on Conductivity in PEO-$LiBF_4$-40 wt% Li_3N Material.

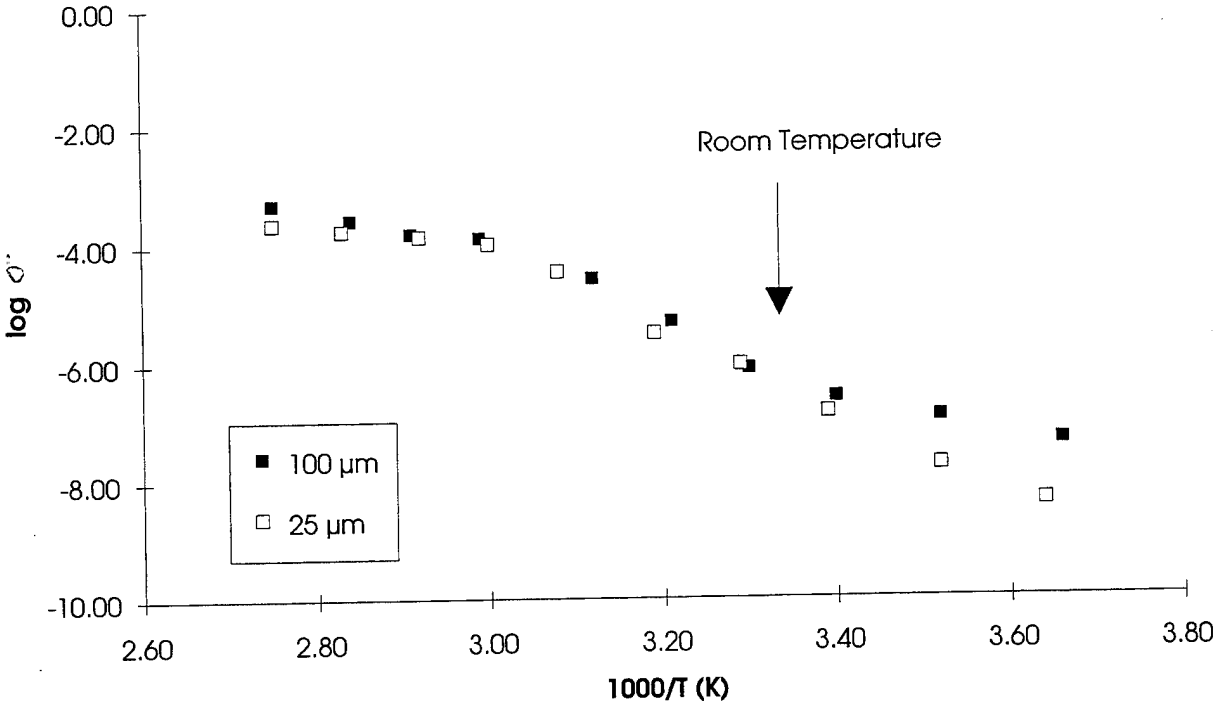

Figure 25. Effect of Li_3N Particle Size on Conductivity in PEO-$LiBF_4$-60 wt% Li_3N Material.

Table 5 presents effects of the first factor. The table also includes compositions, ambient temperature conductivity as measured by the ac impedance technique, and the activation energy for conductivity in the 273-323K range. It is apparent that at lower concentrations of Li_3N, there is a significant increase in conductivity. However, there appears to be little change in conductivity beyond 40% Li_3N. The activation energies for the 40, and 50 percent Li_3N materials also show an inconsistent trend. It may be recalled that the ac impedance spectra of these composite materials show unusual features, and an estimate of conductivity values from these spectra may have some limitations.

The plots of log σ versus 1/T for the 5, 25, and 40 percent Li_3N composite materials are shown in Figure 26. It should be noted that the conductivity increases not only at the ambient temperature but also over the entire temperature range as more Li_3N is added. In addition, there appears to be two distinct regions in the log σ versus 1/T plots, suggesting two different conductivity mechanisms in the 0-100°C temperature range. In the low temperature range, 0-65°C, it is believed that the PEO:$LiBF_4$ complex is in solid state and the activation energy for conductivity is approximately $\cong$30 kcal mole^{-1}. In the higher temperature range, 65-100°C, the major fraction of the electrolyte is in liquid state, which is conducive for high ionic conductivity and low activation energy, 6.1 kcal mole^{-1}.

3.9 Theoretical Basis for Conductivity Enhancement in Li_3N-PEO:$LiBF_4$ Composites

Three major factors need to be considered to explain the high conductivity of PEO:$LiBF_4$-Li_3N composite electrolytes: (a) the additive nature of conductivity, (b) the existence of grain boundaries or solid-solid interfaces, and (c) the Li_3N-induced amorphous structure of the PEO:$LiBF_4$ complex. These factors are further explained in the subsequent paragraphs.

1. Additive Nature of Conductivity

The basic postulate of this factor is that if two phases, one with higher conductivity and another with lower conductivity, are mixed together and the primary conducting ions are the same in the two phases, the conductivity of the mixed phases will have an intermediate value between the two extreme values of conductivity corresponding to the two phases. According to this postulate, the conductivity of the composite electrolyte should increase as the volume fraction of the high conductivity phase Li_3N is increased.

The room temperature conductivities of Li_3N and PEO:$LiBF_4$ (0;Li=8) are reported to be 10^{-3} and 10^{-7} S cm^{-1}, respectively. The diffusion coefficients corresponding to these conductivities can be estimated using the Nerst-Einstein equation. The volume fractions of Li_3N and the PEO:$LiBF_4$ complex in combination with their respective diffusion coefficients yield the

TABLE 5

Composition and Properties of PEO:$LiBF_4$/Li_3N Composite Electrolytes

Specimen No.	Material Composition	log σ at 300K	Activation Energy, ΔE 273-323K	Remarks
1	95% PEO:$LiBF_4$ 5% Li_3N	$1.6x10^{-7}$ S cm^{-1}	27.61 KCal $mole^{-1}$	Easy processing
2	75% PEO:$LiBF_4$ 25% Li_3N	$1x10^{-6}$ S cm^{-1}	27.20 KCal $mole^{-1}$	Easy processing
3	60% PEO:$LiBF_4$ 40% Li_3N	$3x10^{-6}$ S cm^{-1}	38.81 KCal $mole^{-1}$	
4	50% PEO:$LiBF_4$ 50% Li_3N	$2x10^{-6}$ S cm^{-1}	28.04 KCal $mole^{-1}$	
5	40% PEO:$LiBF_4$ 60% Li_3N	$5x10^{-6}$ S cm^{-1}	---	Material was brittle and difficult to handle

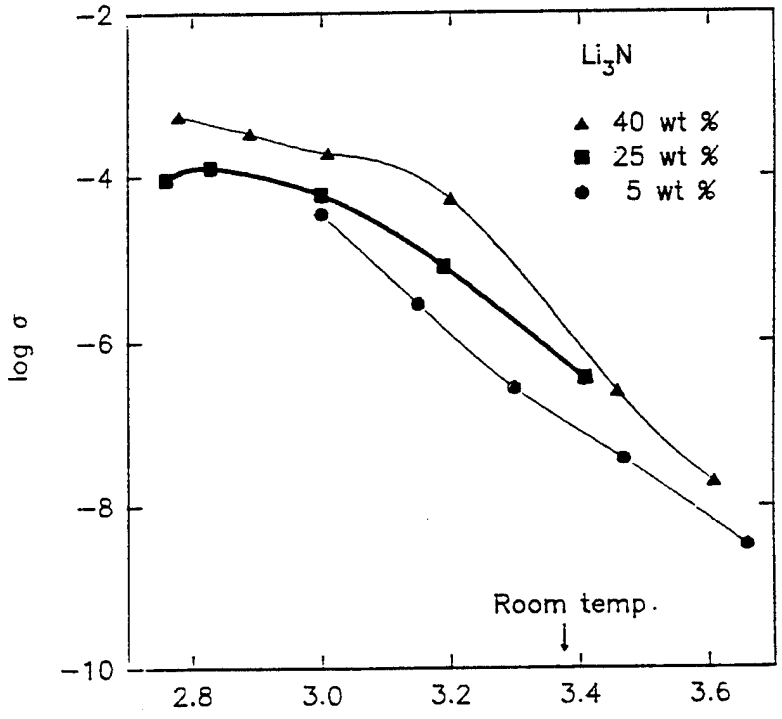

Figure 26. Log σ vs 1/% Plots of PEO:$LiBF_4$ and 5, 25, and 40 wt% Li_3N Materials.

diffusion coefficient of the composite, D_c, which can then be converted to the conductivity of the composite, σ_c, again by using the Nerst-Einstein equation. These parameters for the various volume fractions of the two phases are shown in Table 6. A theoretical plot of log σ versus the volume fraction of Li_3N is shown in Figure 27. It should be noted from Figure 27 that the conductivity of the composite electrolyte increases for all volume fractions of Li_3N; however, remarkable increases are achieved only at very high concentrations of Li_3N.

2. Solid-Solid Interfaces/New Phase

The Li_3N particles are embedded in a matrix of the PEO:$LiBF_4$ complex. The difference in chemical potential between the surfaces of Li_3N and the PEO:$LiBF_4$ materials in contact with each other provides a driving force for the transport of lithium across the grain boundary. In addition to this chemical potential, small particles of Li_3N provide a large area of curved interfaces. The curved interfaces are generally associated with a vapor pressure difference which may also assist diffusional processes and ionic conductivity. The interfaces may also act as traps for anionic species and for impurities such as OH^- groups in PEO.

The chemical reactivity between PEO and Li_3N, particularly at elevated temperatures during annealing results in the formation of a new phase which has a positive influence on the conductivity. The new phase is believed to be three dimensional and interconnected.

3. Amorphous Structure

In the literature it has often been stated that polymers with an amorphous structure are desirable for their conductivity. It has also been reported that the incorporation of a ceramic solid, $LiAlO_2$ (Ref. 4), induces an amorphous structure in PEO-based electrolytes. In view of these suggestions, it is believed that Li_3N would enhance the amorphous structure and, thus, the conductivity of the composite electrolyte.

3.10 Conductivity of Over-Annealed Specimens

In view of the aforementioned discussions, it is reasonable to expect an enhancement in conductivity due to a Li_3N addition. All three factors, the additive nature of conductivity, grain boundaries, and amorphicity, are believed to contribute, but the existence of a new phase is possibly the primary contributor.

The limiting factor of conductivity in under-annealed specimens remains the polymer layer between the Li_3N crystallites. The average thickness, t, is normally calculated by using Eq. (1):

$$t = \frac{(1 - v)r}{3v} \qquad (1)$$

TABLE 6

Conductivity and Diffusion Coefficients of Li_3N, PEO:$LiBF_4$, and Composite Electrolytes

Specimen No.	σ_i S cm^{-1}	σ_p S cm^{-1}	D_i	D_p	V_i	V_p	D_c	σ_c
1	10^{-3}	10^{-7}	$1.6x10^{-6}$	$1.6x10^{-10}$	0.1	0.9	$1.78x10^{-10}$	$2.85x10^{-7}$
2	10^{-3}	10^{-7}	$1.6x10^{-6}$	$1.6x10^{-10}$	0.2	0.8	$2.00x10^{-10}$	$3.2x10^{-7}$
3	10^{-3}	10^{-7}	$1.6x10^{-6}$	$1.6x10^{-10}$	0.3	0.7	$2.29x10^{-10}$	$3.66x10^{-7}$
4	10^{-3}	10^{-7}	$1.6x10^{-6}$	$1.6x10^{-10}$	0.4	0.6	$2.67x10^{-10}$	$4.27x10^{-7}$
5	10^{-3}	10^{-7}	$1.6x10^{-6}$	$1.6x10^{-10}$	0.5	0.5	$3.2x10^{-10}$	$5.12x10^{-7}$
6	10^{-3}	10^{-7}	$1.6x10^{-6}$	$1.6x10^{-10}$	0.6	0.4	$4.0x10^{-10}$	$6.4x10^{-7}$
7	10^{-3}	10^{-7}	$1.6x10^{-6}$	$1.6x10^{-10}$	0.7	0.3	$5.33x10^{-10}$	$8.53x10^{-7}$
8	10^{-3}	10^{-7}	$1.6x10^{-6}$	$1.6x10^{-10}$	0.8	0.2	$8.0x10^{-10}$	$1.28x10^{-6}$
9	10^{-3}	10^{-7}	$1.6x10^{-6}$	$1.6x10^{-10}$	0.9	0.1	$1.6x10^{-9}$	$2.56x10^{-6}$
10	10^{-3}	10^{-7}	$1.6x10^{-6}$	$1.6x10^{-10}$	1.0	0	$1.6x10^{-6}$	10^{-3}
11	10^{-3}	10^{-7}	$1.6x10^{-6}$	$1.6x10^{-10}$	0	1	$1.6x10^{-10}$	10^{-7}

σ = conductivity (S cm^{-1})

D = diffusion coefficients (cm^2sec^{-1})

V = volume fraction

I = Li_3N

P = PEO:$LiBF_4$

C = PEO:$LiBF_4$-Li_3N composite

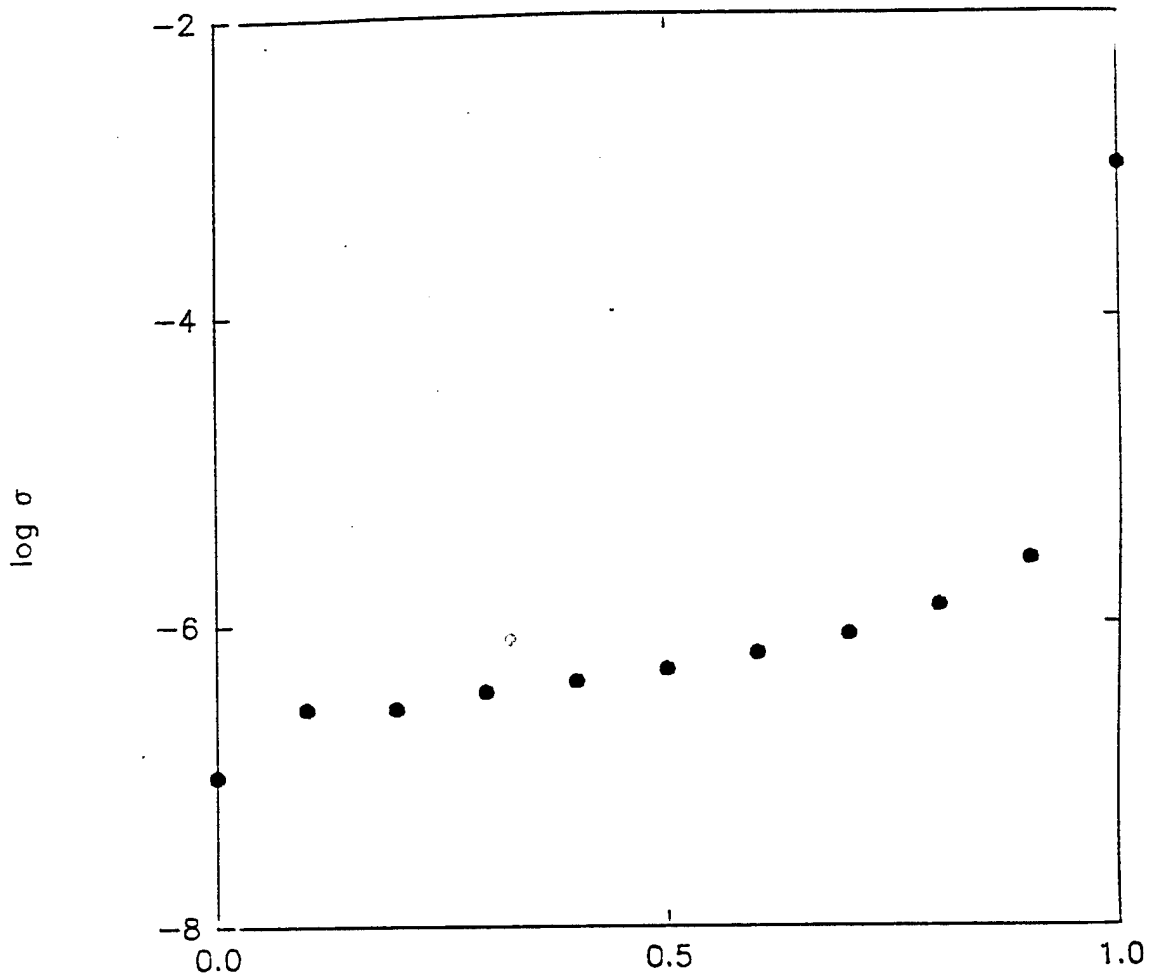

Figure 27. Conductivity of Li_3N-PEO:$LiBF_4$ Composite Electrolyte vs Volume Fraction of Li_3N.

where ν is the volume fraction of crystalline grains of radius, r. For the composite electrolyte with 50 wt% Li_3N and with a mean particle size of 25 μm, the average polymer film thickness turns out to be 10 μm. This polymer film of 10 μm thickness and Li_3N participate in the formation of high conductivity phase when annealed at high temperatures. The phase must exist in a three dimensional, interconnected network to facilitate conduction process. It is quite apparent that volume fraction of Li_3N and its particle size, annealing temperature, time and atmosphere, and other reaction initiating components are critical parameters and need to be carefully investigated to optimize processing and properties of PEO-Li_3N composite materials.

X-ray diffraction has shown that not all Li_3N is consumed during annealing; a residual Li_3N phase remains. A single crystal of Li_3N exhibits anisotropy in conductivity. However, in PEO:$LiBF_4$-Li_3N composite electrolytes, Li_3N crystallites are randomly oriented and, in combination with the matrix phase, are expected to produce a material with isotropic ionic conductivity, although some measurements need to be performed to verify the hypothesis.

4. SUMMARY AND CONCLUSIONS

1. A processing technique to produce ≅100 μm thick films of PEO:$LiBF_4$-Li_3N composite electrolyte was developed. The electrochemical properties of the film were found to be sensitive to annealing temperature and time.

2. The ac impedance technique was used to characterize the composite films. At low concentrations of Li_3N, the electrolytes exhibited interpretable ac impedance spectra; however, at higher Li_3N concentrations the spectra were complex. Nonetheless, the general observation was that the increasing concentration of Li_3N increased the conductivity of the composite electrolyte.

3. Annealing of specimens in 125-145°C temperature range yields high conductivity material. The reproducibility of the specimen preparation and conductivity data is excellent.

4. Characterization of the specimen using DSC, TGA, x-ray diffraction, and infrared spectroscopy reveal that a high temperature (125-145°C) annealing leads to formation of a new phase which is believed to be the high conductivity phase.

5. Cyclic voltammograms obtained from the composite electrolyte material reveal that these materials are stable when in contact with lithium.

6. A symmetric Li/composite electrolyte/Li cell was cycled successfully for 150 cycles with a current density of 100 μA cm^{-2}.

5. REFERENCES

1. K.M. Abraham and N. Alamgir, 'Li$^+$-Conductive Solid Polymer Electrolytes With Liquid-like Conductivity," *J. Electrochem. Soc.* **137**, 1657 (1990).

2. J.E. Weston and B.C.H. Steele, "Effects of Inert Fillers on the Mechanical and Electrochemical Properties of Lithium Salt-poly(ethylene oxide) Polymer Electrolytes," *Solid State Ionics* 7, 75 (1982).

3. F. Capuano, F. Croce, and B. Scrosati, "Composite Polymer Electrolytes," *J. Electrochem. Soc.* **138**, 1918 (1991).

4. F. Groce, F. Gerace, and B. Scrosati, "Interfacial Phenomenon in Lithium Polymer Electrolyte Batteries," Proceedings of the 35th International Power Sources Symposium, Cherry Hill, NJ, June 22-25, pp. 267-270 (1992).

5. N. Munichandraiah, L.G. Scanlon, R.A. Marsh, B. Kumar, and A.K. Sircar, "Studies on the Composite Polymer Electrolyte of Poly(ethylene oxide) and Zeolite," Proceedings of Electrochemical Society, Honolulu, HI (May 1993).

6. B. Kumar, J.D. Schaffer, and M. Nookala, "Electrochemical Performance of PEO:$LiBF_4$ and PEO:$LiBF_4$-Glass Composite Electrolytes," Proceedings of the 18th International Power Sources Symposium, Stratford-upon-Avon, England (April 1993).

7. U.V. Alpen, A. Rabenau, and G.H. Talat, "Ionic Conductivity of Li_3N Single Crystals," *Appl. Phys. Lett.* **20**, 621 (1977).

8. S. Skaarup, K. West, and B. Zachau-Christiansen, "Mixed Phase Solid Electrolytes," *Solid State Ionics*, **28-30**, 975 (1988).

9. S. Yang, P. Yao, T. Lee, and C. Chang, "Electrochemical Properties of Li_3N Polycrystalline Electrolytes at High Temperatures," Proceedings of 15th International Power Sources Symposium, Brighton, England (September 1986), p. 16.